Received: 13 August 2018 | Revised: 20 December 2018 | Accepted: 8 January 2019

DOI: 10.1002/cne.24634

WILEY JCN RESEARCH IN SYSTEMS NEUROSCIENCE THE JOURNAL OF COMPARATIVE NEUROLOGY

RESEARCH ARTICLE

Both excitatory and inhibitory neurons transiently form clusters at the outermost region of the developing mammalian cerebral neocortex

Minkyung Shin[1] | Ayako Kitazawa[1] | Satoshi Yoshinaga[1] | Kanehiro Hayashi[1] | Yukio Hirata[1] | Colette Dehay[2] | Ken-ichiro Kubo[1] | Kazunori Nakajima[1]

[1]Department of Anatomy, Keio University School of Medicine, Tokyo, Japan

[2]Inserm, Stem Cell and Brain Research Institute U1208, Université de Lyon, Université Claude Bernard Lyon 1, Bron, France

Correspondence
Kazunori Nakajima and Ken-ichiro Kubo, Department of Anatomy, Keio University School of Medicine, 35 Shinanomachi, Shinjuku-ku, Tokyo 160-8582, Japan.
Emails: kazunori@keio.jp; kkubo@keio.jp

Funding information
FRM Equipe, Grant/Award Number: DEQ20160334943; Grants-in-Aid for Scientific Research (KAKENHI) of the Ministry of Education, Culture, Sports, Science and Technology (MEXT) and Japan Society for the Promotion of Science, Grant/Award Numbers: JP15H02355, JP15K06745, JP16H06482, JP16K09997, JP18K06842, JP18K07855, JP18K19379; Kawano Masanori Memorial Public Interest Incorporated Foundation for Promotion of Pediatrics; Keio Gijuku Academic Development Funds; Keio Gijuku Fukuzawa Memorial Fund for the Advancement of Education and Research; LABEX CORTEX, Grant/Award Number: ANR-11-LABX-0042; Naito Foundation; NOVARTIS Foundation (Japan) for the Promotion of Science; Primacor, Grant/Award Number: ANR-14-CE13-0036; Takeda Science Foundation

Abstract

During development of the mammalian cerebral neocortex, postmitotic excitatory neurons migrate toward the outermost region of the neocortex. We previously reported that this outermost region is composed of densely packed relatively immature neurons; we named this region, which is observed during the late stage of mouse neocortical development, the "primitive cortical zone (PCZ)." Here, we report that postmigratory immature neurons spend about 1–1.5 days in the PCZ. An electron microscopic analysis showed that the neurons in the PCZ tend to be in direct contact with each other, mostly in a radial direction, forming "primitive neuronal clusters" with a height of 3–7 cells and a width of 1–2 cells. A time-course analysis of fluorescently labeled neurons revealed that the neurons took their positions within the primitive clusters in an inside-out manner. The neurons initially participated in the superficial part of the clusters, gradually shifted their relative positions downward, and then left the clusters at the bottom of this structure. GABAergic inhibitory interneurons were also found within the primitive clusters in the developing mouse neocortex, suggesting that some clusters are composed of both excitatory neurons and inhibitory interneurons. Similar clusters were also observed in the outermost region of embryonic day (E) 78 cynomolgus monkey occipital cortex and 23 gestational week (GW) human neocortices. In the primate neocortices, including human, the presumptive primitive clusters seemed to expand in the radial direction more than that observed in mice, which might contribute to the functional integrity of the primate neocortex.

KEYWORDS

excitatory neuron, *in utero* electroporation (IUE), inhibitory interneuron, mammalian neocortical development, neuronal migration, primate neocortical development, primitive cortical zone (PCZ), primitive neuronal clusters, RRID: AB_10712211, AB_141607, AB_141708, AB_141709, AB_162542, AB_162543, AB_2068506, AB_2298772, AB_2340375, AB_2491093, AB_2535853, AB_2536180, AB_2539796, AB_300798, AB_305426, AB_634520

1 | INTRODUCTION

Mammalian neocortex is organized into a six-layered laminar structure composed of both excitatory and inhibitory neurons. All cortical excitatory neurons are generated directly or indirectly from the progenitors within the ventricular zone (VZ), which lines the surface of the dorsal wall of the lateral ventricle, whereas inhibitory interneurons originate from progenitors within the germinal zones of the ventral telencephalon. Both types of newly generated neurons migrate away from where they are born to where they permanently settle.

The first generated cells during corticogenesis form the preplate, which splits and differentiates into the marginal zone (MZ) and the

Minkyung Shin and Ayako Kitazawa contributed equally to this study.

subplate after newly born excitatory neurons start to migrate toward the pial surface (Hirota & Nakajima, 2017). The neuronal migration is guided by a scaffold called radial fibers of the radial glial cells, which extend to the pial surface (Rakic, 1972, 1988). The neurons terminate their migration when they reach beneath the MZ, forming a cortical plate (CP) in a birth-date-dependent and inside-out manner; that is, earlier-born neurons ultimately occupy deep layers, whereas later-born neurons pass the earlier-born neurons to inhabit the superficial layers (Angevine & Sidman, 1961; Greig, Woodworth, Galazo, Padmanabhan, & Macklis, 2013; Tan & Shi, 2013). The vast majority of the inhibitory interneurons migrates tangentially and is incorporated into the CP with a mild inside-out neurogenesis gradient (Anderson, Eisenstat, Shi, & Rubenstein, 1997; Rymar & Sadikot, 2007; Taniguchi, Lu, & Huang, 2013; Yozu, Tabata, & Nakajima, 2004).

The extracellular protein Reelin, which is secreted mainly by Cajal–Retzius cells within the MZ, is a key molecule causing the proper organization of the cortical layers during neocortical development (Bar et al., 1995; Caviness & Sidman, 1973; D'Arcangelo et al., 1995; Hayashi, Inoue, & Nakajima, 2018; Hirota & Nakajima, 2017; Honda, Kobayashi, Mikoshiba, & Nakajima, 2011; Ogawa et al., 1995). Analyses of the neocortex in the autosomal recessive mutant mouse *reeler*, which lacks the Reelin molecule, revealed that Reelin is required for the inside-out pattern of neuronal alignment. Although Reelin controls multiple aspects of neocortical development, the mechanisms of Reelin function have not been completely understood. One of the important functions of Reelin is that it can cause neuronal aggregation both *in vitro* and *in vivo* (Hirota, Kubo, Fujino, Yamamoto, & Nakajima, 2018; Ishii et al., 2015; Kohno et al., 2015; Kubo et al., 2010; Matsunaga et al., 2017). Notably, the ectopic overexpression of Reelin in the developing neocortex causes neuronal aggregation in a birth-date-dependent manner (Kubo et al., 2010), suggesting that this aggregation is a properly controlled phenomenon rather than simple aggregation.

Moreover, we found that the outermost region of the CP in the developing wild-type neocortex, but not in the *reeler* neocortex, is composed of densely packed relatively immature neurons, which are still negative for the mature neuronal marker NeuN, resembling the neuronal aggregates induced by ectopic Reelin overexpression. Therefore, we designated this zone of densely packed relatively immature neurons at the outermost region of the CP as the "primitive cortical zone (PCZ)" (Sekine et al., 2012; Sekine, Honda, Kawauchi, Kubo, & Nakajima, 2011; Sekine, Kubo, & Nakajima, 2014). Since the PCZ is observed only around E16.5 to P3.5 in developing mouse neocortex, this phenomenon is thought to be restricted to developmental stages. However, how each excitatory neuron participates in and later leaves the PCZ and what kind of neurons compose the PCZ (e.g., whether or not GABAergic interneurons are also involved) remain unclear. In this study, we investigated (a) the birth-date profiles of the neuronal positioning and formation of "primitive neuronal clusters" in and beneath the PCZ in the developing mouse neocortex using *in utero* electroporation (IUE) and electron microscopic (EM) analysis, (b) the participation of GABAergic interneurons in the primitive neuronal clusters with direct contact with excitatory neurons, and (c) the presumptive primitive neuronal clusters in the outermost region of the CP in embryonic day (E) 78 macaque and 23 gestational week (GW) human neocortices.

2 | MATERIALS AND METHODS

2.1 | Animals

All the mouse experiments were conducted in accordance with the Keio University Institutional Animal Care and Use Committee, Institutional Guidelines on Animal Experimentation, Japanese Government Law Concerning the Protection and Control of Animals, and Japanese Government Notification of Feeding and Safekeeping of Animals. Pregnant ICR mice were purchased from Japan SLC (Shizuoka, Japan). Mice were housed under a 12-hr light/12-hr dark cycle in a temperature-controlled room and were given free access to food and water. The day of vaginal plug detection was considered to be embryonic day 0.5 (E0.5). Experiments performed before and after 12 p.m. of embryonic day x (Ex) were considered as Ex and Ex.5, respectively. Embryonic day 19.0 was designated as postnatal day 0 (P0).

The cynomolgus monkey (*Macaca fascicularis*) facility and all the experimental protocols involving nonhuman primates were approved by the Animal Care and Use Committee CELYNE (C2EA#42). The animals were housed in a controlled environment (temperature: 22 ± 1 °C) with a 12-hr light/12-hr dark cycle (lights on at 8 a.m.). All animals were given a commercial monkey diet twice a day with tap water ad libitum and were fed fruits and vegetables once daily. During and after the experiments, the monkeys remained under careful veterinary oversight to ensure good health. Fetuses from timed-pregnant cynomolgus monkey (E78—gestation period of 165 days) (*M. fascicularis*) were delivered by caesarean section according to the protocols described by Lukaszewicz et al. (2005). The surgical procedures and animal experimentation were in accordance with European requirements 2010/63/UE. Protocols C2EA42-12-11-0402-003 and APAFIS#3183 have been approved by the Animal Care and Use Committee CELYNE (C2EA #42).

2.2 | *In utero* electroporation

Pregnant ICR mice were deeply anesthetized with pentobarbital sodium (Nembutal), and their intrauterine embryos were surgically manipulated as described previously (Nakajima, Mikoshiba, Miyata, Kudo, & Ogawa, 1997; Tabata & Nakajima, 2001, 2008). A plasmid solution volume of 1–2 μL was injected into the lateral ventricles, and IUE was performed. The plasmid solution contained 1 mg/mL of CAG-driven enhanced green fluorescent protein (EGFP) expression vectors (pCAGGS-EGFP) and 0.01% fast green solution. The electronic pulse conditions on E14.5 were 34 V, 50 ms, and four times; the pulses were applied using an electroporator (CUY-21 or NEPA21; NEPAGENE) with a forceps-type electrode (CUY650P5). Sequential IUE was performed using pCAGGS-EGFP and CAG-driven tdTomato protein (tdTomato) expression vectors (pCAG-tdTomato) at a 1-day interval. The electronic pulses were loaded using the above conditions on both E14.5 and E15.5.

2.3 | Preparation of frozen brain sections

Coronal slices of developing mouse cerebral cortex were prepared as described previously (Tabata & Nakajima, 2003). Briefly, the embryos and neonates were placed on ice for anesthesia and their brains were

TABLE 1 Primary and secondary antibodies used in this study

Antibody	Immunogen	Manufacturing details	RRIDs	Dilution
Primary antibodies				
Anti-BrdU		Rat, monoclonal, Abcam, #ab6326	AB_305426	1:500
Anti-calbindin	C-terminal of human calbindin D28K	Goat, polyclonal, Santa Cruz, #SC-7691	AB_634520	1:1000
Anti-calretinin	Recombinant rat calretinin	Rabbit, Millipore, #AB5054	AB_2068506	1:1000
Anti-GFP	Recombinant full-length protein corresponding to GFP	Chick, polyclonal, Abcam, #ab13970	AB_300798	1:500
Anti-GFP	Synthetic peptides (NC_011521)	Rabbit, polyclonal, Frontier institute, #FRL-GFP-RB-AF2020	AB_2491093	1:200
Anti-NeuN	Purified cell nuclei from mouse brain; clone A60	Mouse, monoclonal, Millipore, #MAB377	AB_2298772	1:100
Anti-Prox1	Recombinant fragment corresponding to Human PROX1 (C-terminal)	Rabbit, polyclonal, Abcam, #ab101851	AB_10712211	1:1000
Secondary antibodies				
Anti-chicken IgY (IgG) (H + L), Alexa Fluor 488 conjugated		Donkey, polyclonal, Jackson, #703-545-155	AB_2340375	1:200
Anti-goat IgG (H + L), Alexa Fluor 555 conjugated	Gamma immunoglobins heavy and light chains	Donkey, polyclonal, Invitrogen, #A21432	AB_2535853	1:500
F(ab′)2-goat anti-rabbit IgG (H + L), nanogold conjugated	Gamma immunoglobin	Goat, polyclonal, Molecular Probes, #N-24916	AB_2539796	1:200
Anti-mouse IgG (H + L), Alexa Fluor 488 conjugated	Gamma immunoglobins heavy and light chains	Donkey, polyclonal, Invitrogen, #A21202	AB_141607	1:500
Anti-mouse IgG (H + L), Alexa Fluor 555 conjugated	Gamma immunoglobins heavy and light chains	Donkey, polyclonal, Invitrogen, #A31570	AB_2536180	1:500
Anti-mouse IgG (H + L), Alexa Fluor 647 conjugated	Gamma immunoglobins heavy and light chains	Donkey, polyclonal, Invitrogen, #A31571	AB_162542	1:500
Anti-rabbit IgG (H + L), Alexa Fluor 488 conjugated	Gamma immunoglobins heavy and light chains	Donkey, polyclonal, Invitrogen, #A21206	AB_141708	1:500
Anti-rabbit IgG (H + L), Alexa Fluor 555 conjugated	Gamma immunoglobins heavy and light chains	Donkey, polyclonal, Invitrogen, #A31572	AB_162543	1:500
Anti-rat IgG (H + L), Alexa Fluor 488 conjugated	Gamma immunoglobins heavy and light chains	Donkey, polyclonal, Invitrogen, #A21208	AB_141709	1:500

Research resource identifiers = RRIDs.

collected into 4% paraformaldehyde (PFA) in a 0.1-M sodium phosphate buffer (pH 7.4). The brains were postfixed overnight at 4 °C. After sequential cryoprotection in 20 and 30% sucrose (in phosphate-buffered saline), the brains were embedded in Optical Cutting Temperature (O.C.T.) compound (Sakura, Tokyo, Japan) and frozen using liquid nitrogen.

A lethally anesthetized macaque fetus (via intraperitoneal injection with sodium pentobarbital, 60 mg/kg) at E78 was perfused through the heart with buffered 4% PFA for 30 min. After sequential cryoprotection in 10 and 20% sucrose (in phosphate buffer), the brain was embedded in Tissue-Tek. Then, 20-μm-thick parasagittal cryosections were obtained using a cryostat (Microm, HM550; Thermo Fisher Scientific, Waltham, MA), mounted on Superfrost glass slides (Superfrost Plus; Thermo Fisher Scientific), and stored at −20 °C.

2.4 | Immunohistochemistry

After restoring the frozen mouse and monkey brain sections to room temperature (RT), the sections were treated with an antigen retrieval reagent (HistoVT One, 06380-05; Nacalai Tesque, Kyoto, Japan) for 20 min at 70 °C. After washing three times with PBS for 10 min each, the sections were incubated with 10% normal donkey serum in PBS-Tx for 1 hr at RT and then with the primary antibodies overnight at 4 °C. After washing with 0.01% Triton X-100 (Sigma-Aldrich, St. Louis, MO) in PBS (PBS-Tx) for three times, the sections were incubated with secondary antibodies for 1 hr at RT. The details of the antibodies and stains are shown in Table 1. Nuclear staining was performed using 4′,6-diamidino-2-phenylindole (D3571; Thermo Fisher Scientific) when applying the secondary antibodies. Mounting was realized in PermaFluor aqueous mounting medium (TA-030-FM; Thermo Fisher Scientific). The fluorescence images were acquired through confocal laser scanning microscopes (FV1000; Olympus, Tokyo, Japan & TCS SP8; Leica, Wetzlar, Germany) or a fluorescence microscope (BZ-9000; Keyence, Osaka, Japan).

2.5 | Time-lapse imaging

Time-lapse imaging was performed as described previously (Kitazawa et al., 2014; Tabata & Nakajima, 2003). Briefly, the sequential IUE was performed with pCAGGS-EGFP into the ICR mouse cortex at E13.0, and then with pCAG-tdTomato into the cortex at E14.0. Three days later, the brains were embedded in 3% low-melting temperature agarose (SeaPlaque Agarose, 50100; Cambrex, East Rutherford, NJ) and cut with a vibratome (VT1000S; Leica). Coronal brain slices (300-μm thick) were placed on a Millicell-CM membrane (pore size, 0.4 μm; Merck Millipore, Burlington, MA) set on a glass-base dish (AGC

Techno Glass, Shizuoka, Japan). Slices were cultured in Neurobasal medium containing 2% B27 (17504044; Thermo Fisher Scientific), 10% FBS, 0.5% penicillin–streptomycin (15140; Thermo Fisher Scientific) and 500 μM L-glutamine (25030081; Thermo Fisher Scientific). The dishes were then incubated in a 5% CO_2 and 40% O_2 providing chamber fitted on a confocal microscope (FV1000; Olympus). Approximately 10 optical Z-sections were acquired every 30 min, and a movie was created after all the planes were projected as a single image. In the GAD67-GFP mice, IUE was performed with pCAG-tdTomato into the GAD67-GFP mouse cortex at E14.5. Five days later, the brains were collected and prepared for time-lapse imaging in the same manner as described above. The images were acquired every 20 min using a confocal microscope (TCS SP8; Leica).

2.6 | Electron microscopy

P0 C57BL/6N and E18.0 ICR mice were perfused with 2% (or 4% for ICR mice) PFA, 2.5% glutaraldehyde (G003; TAAB Laboratory and Microscopy, Aldermaston, UK), 0.1% picric acid (27926-02; Nacalai Tesque), and 0.05 mg/mL ruthenium red (R003; TAAB Laboratory and Microscopy) in 0.1-M phosphate buffer (PB, pH 7.2). The brains were removed and postfixed for 1–2 hr at 4 °C in the same fixative solution. After washing with 0.1-M PB, 300-μm-thick coronal brain sections were prepared using a vibratome, and the sections were postfixed in 1% osmium tetroxide (3020, Nisshin EM, Tokyo, Japan) for 30 min at RT. After dehydration with 70, 80, 90, 95, and 100% ethanol solutions and replacement with *n*-butyl glycidyl ether (QY-1, 310-1; Nisshin EM), the sections were embedded in Epon 812 resin (340; Nisshin EM). Ultrathin sections (60–80-nm thick) were obtained using a Leica Ultracut UCT and stained with 2% uranyl acetate and lead citrate. Electron micrographs were obtained using a JEM-1400 (JEOL, Tokyo, Japan). Photoshop software (Adobe Photoshop, San Jose, CA) was used to colorize (magenta and blue) the EM images.

2.7 | Immunoelectron microscopy

E17.0, P1.0 ICR, and P0 GAD67-GFP mice were perfused with fixative solution (4% PFA, 1% glutaraldehyde, and 0.1% picric acid in 0.1-M PB). Their brains were then removed and postfixed for 3–4 hr at 4 °C in the same fixative solution. For the ICR mice, IUE was performed at E14.5 (detailed procedures are described in Section 2.2). After washing with 0.1-M PB, 100-μm thick coronal brain sections were prepared using a vibratome. The brain sections were incubated with blocking solution (5% normal goat serum, 0.005% saponin in 0.1-M PB) for 30 min at RT and then with an anti-rabbit GFP antibody (FRL-GFP-Rb-AF2020; Frontier Institute, Hokkaido, Japan) overnight at RT. After washing with 0.005% saponin in 0.1-M PB, the sections were incubated with a Nanogold Fab' fragment of Goat anti-rabbit IgG (N-24916; Thermo Fisher Scientific) in blocking solution for 90 min at RT. After washing with 0.1-M PB, the sections were incubated with 0.5% glutaraldehyde in 0.1-M PB for 10 min at RT. After washing with 0.1-M PB, the immunoreactive nanogold particles on the brain sections were enhanced using an HQ silver enhancement kit (2012, Nanoprobes, Yaphank, NY) and washed with distilled water under dark conditions. Then, the sections were postfixed with 1% osmium tetroxide for 15 min at RT. After dehydration with a series of ethanol solutions and replacement with QY-1, the sections were embedded in epoxy resin. Ultrathin sections were stained with 2% uranyl acetate for 14 min, followed by lead citrate for 12 min at RT. EM images were obtained in the same manner as described in Section 2.6.

2.8 | Nissl staining

The PFA-fixed mouse brain sections were restored to RT status. Nissl staining was performed using 0.1% cresyl violet according to the standard protocol. The images were acquired through a brightfield imaging color camera (DP80; Olympus) attached to a BX50 microscope (Olympus).

2.9 | 5-Ethynyl-2′-deoxyuridine and 5-bromo-2′-deoxyuridine injection

5-Ethynyl-2′-deoxyuridine (EdU; A10044; Thermo Fisher Scientific) solution (5 mg/mL) and 5-bromo-2′-deoxyuridine (BrdU; B9285; Sigma) solution (10 mg/mL) were prepared by diluting with distilled water. The EdU and BrdU solutions were injected into the abdominal cavity of pregnant mice at a dose of 30 μg EdU/g body weight or 50 μg BrdU/g body weight and were sequentially introduced into E14.5 (EdU) or E15.5 (BrdU) pregnant mice, respectively. The embryos or neonates were collected from E17.5 to P1.5 at 1-day interval. After BrdU immunostaining, EdU staining was performed according to the Click-iT Plus EdU imaging protocol (C10638; Thermo Fisher Scientific).

2.10 | Human fetal brain tissue sections from the "Hirata collection"

Human fetal brains from the "Hirata Collection" were analyzed after obtaining the approval of the institutional review board (Ethics Committee) at Keio University School of Medicine (approval number 20140073). The brains for the tissue sections were collected by Yukio Hirata prior to the 1990s, when he worked at the Tokyo Medical University. The brains were obtained from abortions or autopsies with proper informed consent and were fixed in 10% formalin in saline. After fixation, the brains were processed for celloidin embedding, and microtome sections were cut at 24 μm. Nissl staining was performed using cresyl violet. The brightfield images were acquired through an NY-D5200 Supersystem camera (Nikon, Tokyo, Japan) attached to a microscope (Microscope Network, Kawaguchi, Japan).

3 | RESULTS

3.1 | Neurons transiently participate in the PCZ in the developing mouse neocortex

To clarify the exact temporal profiles of the positioning of neurons that enter and later separate from the PCZ, we introduced an EGFP-expressing plasmid into the lateral ventricle using IUE at E14.5 and collected the brains at half-day intervals after 3–7 days, with the exception of 6.5 days. Since the plasmid was transfected into cells residing along the ventricular surface, most of the labeled cells were expected to share the same birth date (Ajioka & Nakajima, 2005; Hatanaka, Hisanaga, Heizmann, & Murakami, 2004; Tabata, Kanatani, &

Nakajima, 2009). The analysis was performed at the dorsolateral region of the somatosensory cortex, where the hippocampus is located relatively horizontally.

At 3 days after IUE (DIUE), EGFP-labeled neurons had begun to migrate toward the pial surface; many of them had a multipolar morphology in the intermediate zone (IZ) while some in the CP had a

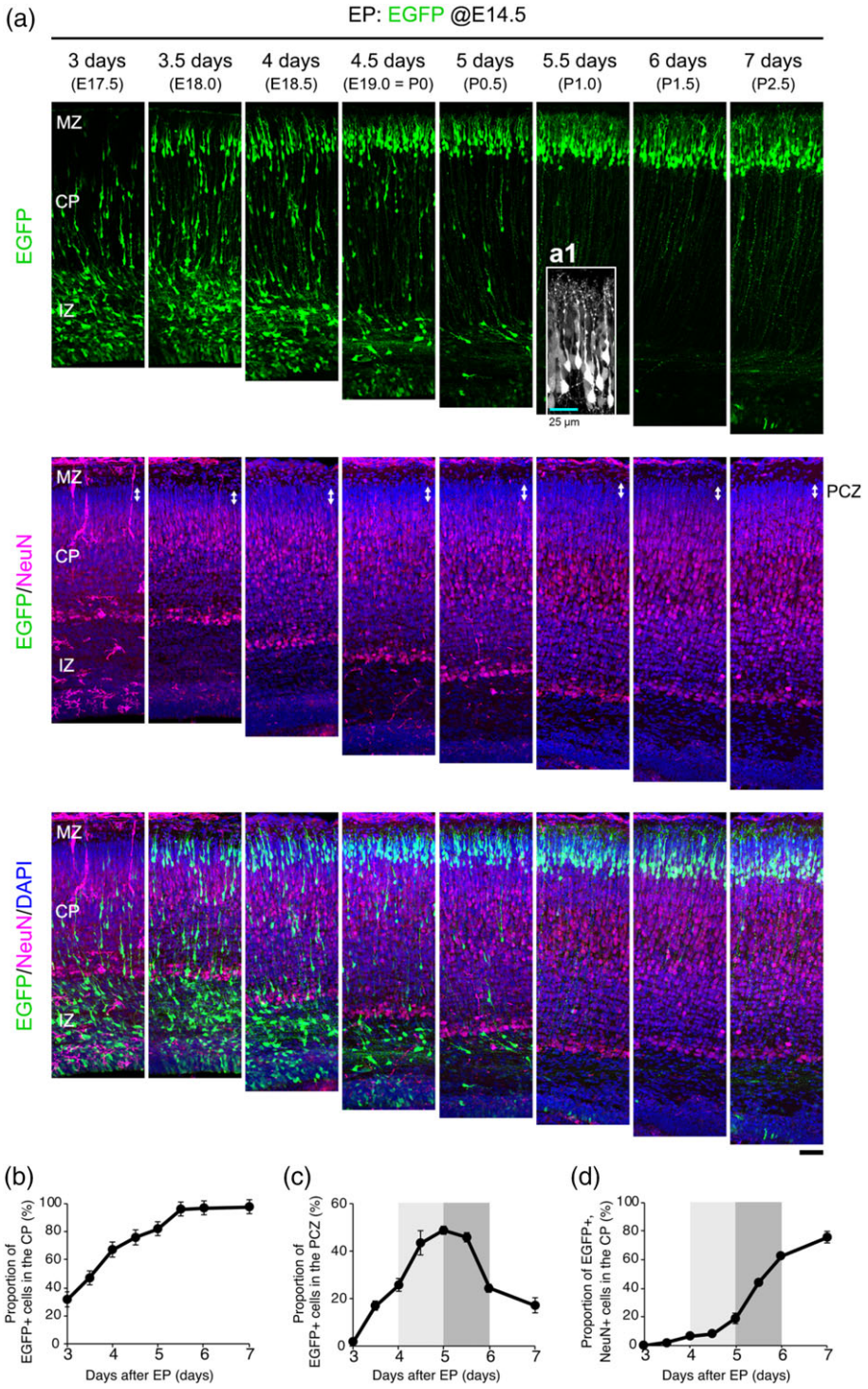

FIGURE 1 Migratory profiles of EGFP-labeled neurons in mouse somatosensory cortex. (a) Brains were obtained at half-day intervals from 3 to 7 days (with the exception of 6.5 days) after the *in utero* electroporation (DIUE) of EGFP at E14.5 and were stained with an anti-NeuN antibody (magenta) and 4′,6-diamidino-2-phenylindole (DAPI; blue). The primitive cortical zone (PCZ) is indicted by the white indicators in the middle panels. (a1) Enlarged view of the EGFP-labeled neurons at 5.5 DIUE. (b–d) The EGFP-labeled cells within the CP and the labeled cells positive or negative for NeuN were counted (n = 3). (b) Proportion of EGFP-positive cells in the CP relative to the total number of EGFP-positive cells found except in the VZ (average ± *SEM*). (c) Proportion of EGFP-positive and NeuN-negative cells in the PCZ relative to the total number of EGFP-positive cells found except in the VZ. (d) Proportion of EGFP-positive and NeuN-positive cells in the CP relative to the total number of EGFP-positive cells found except in the VZ. CP = cortical plate; MZ = marginal zone; IZ = intermediate zone. Scale bar: 50 μm

bipolar shape, indicating that most of the labeled neurons were transitioning from the multipolar to locomotion mode of migration (Figure 1a, 3 days) (Noctor, Martinez-Cerdeno, Ivic, & Kriegstein, 2004; Tabata et al., 2009; Tabata & Nakajima, 2003). At 3.5 DIUE, some of the labeled neurons had already arrived at the top of the CP, while the majority of them were still found in the IZ (Figure 1a, 3.5 days). Early-arrived EGFP-labeled neurons were already found in the PCZ, which was denoted by a NeuN-negative zone beneath the MZ (Figure 1c, 3.5 days, average ± *SEM*: 16.8 ± 2.0%, n = 3 brains). At 4 DIUE, the number of labeled neurons that had reached the PCZ had increased, compared with that on 3.5 DIUE (Figure 1c, 4 days, average ± *SEM*: 25.7 ± 2.7%, n = 3 brains). Even though the population size was quite small, NeuN-positive EGFP-labeled neurons began to be detected below the PCZ (NeuN negative) at this stage (Figure 1d, 4 days, average ± *SEM*: 6.5 ± 1.2%, n = 3 brains). By 4.5 DIUE, a substantial number of EGFP-labeled neurons was found within the PCZ (Figure 1c, 4.5 days, average ± *SEM*: 43.6 ± 5.1%, n = 3 brains). At 5 DIUE, the maximum number of labeled neurons was found within the PCZ (Figure 1c, 5 days, average ± *SEM*: 49.2 ± 1.6%, n = 3 brains). A similar proportion of labeled neurons was observed in the PCZ at 5.5 DIUE. However, the ratio of NeuN-positive EGFP-labeled neurons to the total number of EGFP-labeled neurons was dramatically increased compared with that on 5 DIUE (Figure 1d, 5 days, average ± *SEM*: 19.0 ± 3.9%, n = 3 brains, 5.5 days, average ± *SEM*: 44.0 ± 2.2%, n = 3 brains), demonstrating that EGFP-labeled neurons were in the maturation process. Accordingly, EGFP-labeled apical dendrites that had invaded the MZ were arborized and elongated at 5.5 DIUE (Figure 1a1). At 6 DIUE, the PCZ population had significantly decreased with a steep rise in NeuN-positive EGFP-labeled neurons (Figure 1c, 6 days, EGFP-labeled neurons in the PCZ; average ± *SEM*: 24.4 ± 1.7%, n = 3 brains, Figure 1d, 6 days, NeuN-positive EGFP-labeled neurons; average ± *SEM*: 62.5 ± 1.7%, n = 3 brains), indicating that the major population of EGFP-labeled neurons had matured over these stages. This tendency continued at 7 DIUE (Figure 1c, 7 days, EGFP-labeled neurons in the PCZ; average ± *SEM*: 17.3 ± 3.1%, n = 3 brains, Figure 1d, 7 days, NeuN-positive EGFP-labeled neurons; average ± SEM: 75.6 ± 4.1%, n = 3 brains). Taken together, these results suggest that most of the EGFP-labeled neurons labeled at E14.5 entered the PCZ at 4 to 5 DIUE and became NeuN positive at 5.5 to 6 DIUE while leaving the PCZ, indicating that neurons labeled at E14.5 spend around 1 to 1.5 days in the PCZ.

3.2 | Direct contact between neuronal cell bodies is observed within the neuronal clusters located at the most superficial region of the CP

Although neurons are aligned with a high cell density within the PCZ, whether the neurons are in direct contact with each other remains unknown. Of note, migrating neurons can pass through the PCZ to reach the MZ, even though the cell density is very high in the PCZ. Therefore, we next investigated the detailed structure of the superficial part of the CP, containing the PCZ, using an EM analysis of the developing mouse neocortex at P0.

Low-magnification EM images showed the existence of a cell-dense zone at the top of the CP, which was thought to correspond to the PCZ (Figure 2a). To clarify the cellular organization in the superficial part of the CP, we first indicated some cells in the superficial region of the CP using lowercase letters (Figure 2b) and then confirmed at a higher magnification that the indicated neurons were in direct contact with each other at their cell bodies (Figure 2c) with the exception of one cell (Figure 2b, "p" cell). An analysis of another region is shown in Figure S1, Supporting Information. The cellular relationships of the analyzed cells were designated by drawing indicators that connected neighboring cells when the cells were observed to be in direct contact with each other at their cell bodies (Figure 2d). Then, the angle between this line and the horizontal line tangential to the brain surface was measured. When this angle for pairs of neighboring cells was between 45 and 135° ($45° \leq x < 135°$), the neighboring cells were classified as radially aligned (Figure 2d, magenta color circles). In contrast, if the angle was less than 45° ($0° \leq x < 45°$ or $135° \leq x \leq 180°$), the two cells were considered to be tangentially aligned. If a cell had two neighboring cells with both radial and tangential alignments, the cell was labeled using a half-and-half color (Figure 2d magenta-cyan color circles). To observe the overall appearance of the cellular arrangement, each cell nucleus in Figure 2a was classified according to the above criteria and indicated by a colored circle superimposed on the cell nucleus (Figure S2a, Supporting Information). Cells that seemed to form clusters, at least at this low magnification, were connected by black lines (Figure S2b, Supporting Information). Cells that did not appear to have direct contact with other cells at their cell bodies, at least on the investigated section, were marked in yellow with black circles (Figure S2a,b, Supporting Information).

As a result, we noticed that most of the neurons at the top of the CP tended to be aligned radially, forming clusters extending from beneath the MZ to the superficial part of the CP (Figure S2, Supporting Information). Most of these clusters had a height of 3–7 cells and a width of 1–2 cells. Additionally, tangentially aligned neurons with a width of 2–4 cells were occasionally observed in the superficial part of the CP, including the PCZ. These neurons were frequently found as a part of the radially aligned clusters within the PCZ but were also relatively independently observed beneath the PCZ. Also, the number of isolated cells (yellow with black circles) increased as the cell density decreased toward the deeper part of the CP. Additionally, no significant difference in neuronal alignment was observed between the C57BL/6N and ICR mice (Figure S3, Supporting Information).

To investigate the boundaries between the radially aligned cells in more detail, we next examined the cell–cell relationships at a higher magnification (Figure 3a,b). The cells in the radially aligned clusters (Figure 3a,b, white arrows) below the MZ were indeed in direct contact with each other at their cell bodies (Figure 3a1–a3, b1, b2) and were laterally separated by surrounding structures, such as radial fibers, processes from other neurons, protrusions, etc. (Figure 3a4). Some cells (Figure 3b, blue arrows) positioned beneath the radially aligned cluster were separated from the cluster by intervening structures (Figure 3b3). Cell-membrane-contoured images are shown in Figure S4, Supporting Information. Collectively, these results indicate that the cells positioned at the top of the CP beneath the MZ form clusters with direct cell-to-cell contact and that the cells positioned beneath the clusters may have been

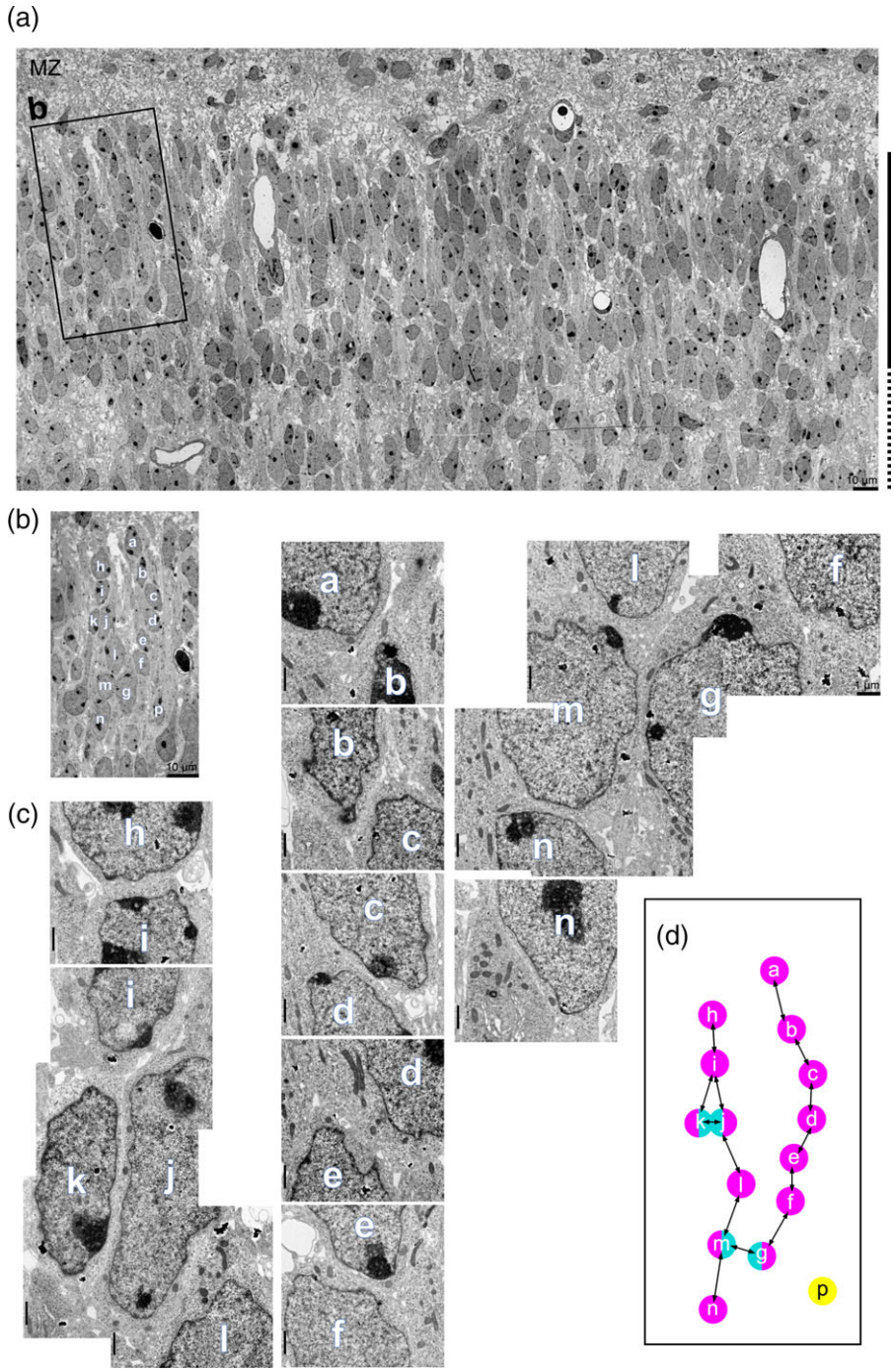

FIGURE 2 Arrangement of the superficial cortical neurons in mouse somatosensory cortex at P0. (a) Coronal view of the neocortex from the MZ to the superficial part of the CP. C57BL/6N mice were analyzed. The presumed primitive cortical zone is indicated by the thick black line next to the figure. (b) Boxed regions in a. The nuclei of the neurons in the panel are indicated by the letters from "a" to "p." (c) Enlarged view of b. (d) The cell nuclei are spotted with magenta (radial), cyan (tangential), or yellow with black circles (isolated) to indicate the relationship with the neighboring cells. Neighboring cells with direct contact with each other at their cell bodies are connected by a black line. MZ = marginal zone

released from the clusters. We propose to call the neuronal clusters in the superficial region of the developing CP, including the PCZ, "primitive neuronal clusters." The neurons in these primitive neuronal clusters tended to be aligned in a radial direction, probably because they were penetrated by radially traversing fibers such as radial glial fibers, leading processes, and the apical dendrites of other neurons, but clustering in a tangential direction was also observed.

3.3 | Migrated neurons are sequentially incorporated into the primitive neuronal clusters and gradually mature

Next, we investigated how neurons change their positions within the primitive clusters during development. Using nuclear staining on single optical sections under a confocal microscope, we were able to identify the radially aligned cells at the top of the CP (Figure 4a,

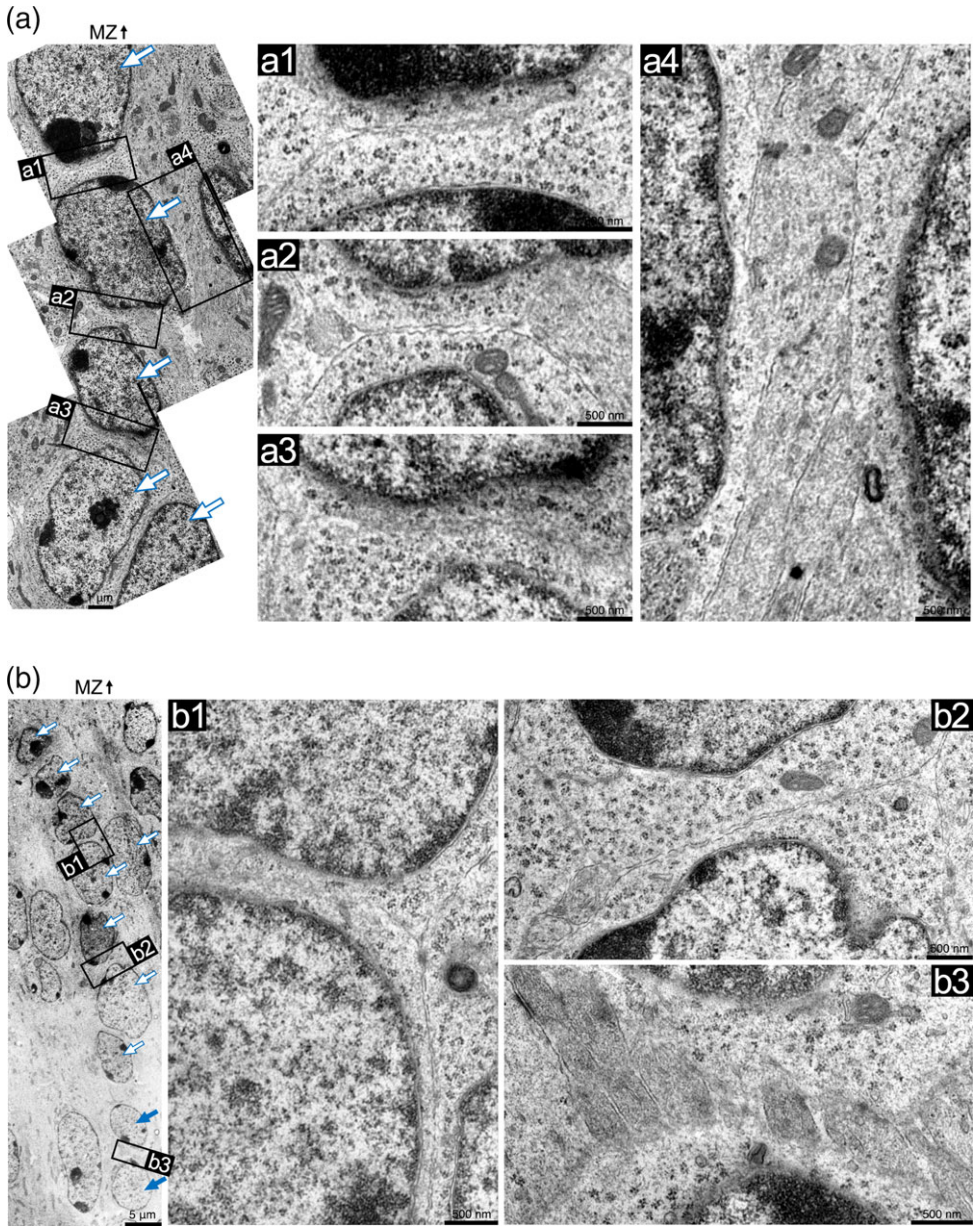

FIGURE 3 High-magnification EM images of primitive neuronal clusters located beneath the MZ in mouse somatosensory cortex at E18.0. (a, b) Coronal view of the neocortex near the MZ. Cells that have direct contact with each other at their cell bodies are indicated by the white arrows, and cells located apart from the cluster are indicated by the blue arrows. (a1–a4, b1–b3) Enlarged views of the boxed regions in a and b. MZ = marginal zone [Color figure can be viewed at wileyonlinelibrary.com]

yellow arrowheads). As shown in the EM analysis (Figure 2 and 3), the volume of the neuronal cytoplasm was quite small, bringing the nuclei of the neighboring cells in the common cluster into very close proximity to each other, especially when forming primitive neuronal clusters. Although determining definitively whether the neurons were in direct contact with each other was difficult using confocal microscopy, we were able to presume the primitive neuronal clusters based on the proximity between nuclei in highly magnified single confocal images. Most EGFP-labeled neurons at 3 DIUE, which were considered to be radially migrating neurons (Figure 1a, 3 days), were observed between the radially aligned presumptive primitive neuronal clusters with a long process extending to the MZ, suggesting that actively migrating neurons are not included in the clusters (Figure 4a, 3 days, white arrows for EGFP-labeled neurons). At 4 DIUE, some EGFP-labeled neurons (Figure 4a, 4 days, designated by a1) were observed to have been incorporated into the top of the presumptive primitive cluster, while the other EGFP-labeled neurons (Figure 4a, 4 days, designated by a2) with a branched leading process, seemingly in the terminal translocation process (Nadarajah, Brunstrom, Grutzendler, Wong, & Pearlman, 2001), were again observed between the clusters. At 5 DIUE, EGFP-labeled neurons were found inside the presumptive primitive clusters. Interestingly, the superficially positioned neurons found within the cluster tended to elongate their apical dendrites along with those of the deeply positioned neurons (Figure 4a, 5 days, denoted with magenta arrows, a3 and a4). This phenomenon was also observed on 7 DIUE (Figure 4a, 7 days, denoted with magenta arrows, a5 and a6). In the end, at 6 and 7 DIUE, the EGFP-labeled neurons were located on the bottom side of the presumptive primitive clusters, and some of them were found apart from the clusters (Figure 4a, 7 days, denoted

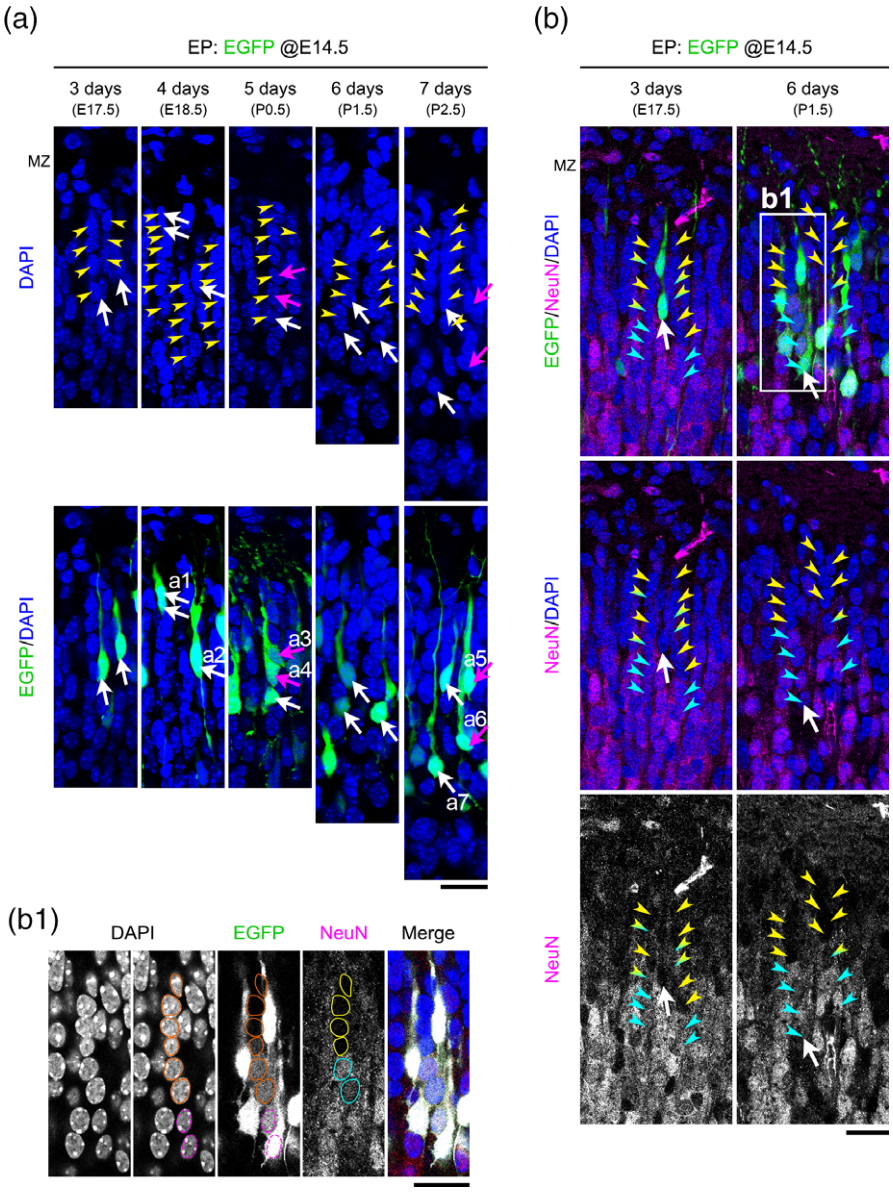

FIGURE 4 Single confocal microscopic images of migrating/migrated neurons with the presumptive primitive neuronal clusters in mouse somatosensory cortex. (a) An EGFP plasmid was electroporated at E14.5 and cortical sections were obtained from 3 to 7 days after the *in utero* electroporation (DIUE) at 1-day interval. The primitive neuronal clusters are indicated by the yellow arrowheads, and EGFP-labeled neurons are indicated by the white or magenta arrows. (b) EGFP-positive migrating and migrated neurons were mainly observed at 3 and 6 DIUE, respectively, and fixed brains were stained with an anti-NeuN antibody. On single optical sections, neurons in the primitive clusters were marked using yellow (NeuN negative), cyan (NeuN positive), or both (relatively weakly NeuN positive)-colored arrowheads. EGFP-labeled neurons are indicated by the white arrows. (b1) High-magnification view of the boxed region in the 6-days panel of (b). The nuclei of the radially clustered neurons are outlined by the orange lines, and the NeuN-negative (yellow) and NeuN-positive (cyan) neurons among them are differentially outlined. The nuclei of neurons at the very bottom of the cluster are outlined by the magenta dotted lines. MZ = marginal zone. Scale bar: 20 μm

with white arrows, a7). These results suggest that the neurons were aligned in an inside-out manner within the clusters.

Since the primitive clusters were observed at the top of the CP, we then examined the relationship between the primitive clusters and the PCZ, which was defined as being composed of NeuN-negative immature neurons (Sekine et al., 2011). At 3 DIUE, EGFP-labeled migrating neurons passing between the presumptive primitive clusters (Figure 4b, 3 days, white arrow) and the superficially located neurons within the clusters were negative for NeuN (Figure 4b, yellow arrowheads), whereas the neurons in the deeper part of the clusters were positive or weakly positive for NeuN (Figure 4b, cyan arrowheads or yellow–cyan gradient arrowheads), indicating that the primitive clusters were composed of both NeuN-negative, weakly-positive, and -positive neurons. On the other hand, at 6 DIUE, most of the EGFP-labeled neurons found in the deeper side of the clusters were NeuN positive (Figure 4b, 6 days, white arrow). Highly magnified single optical sections confirmed that the primitive clusters were composed of both NeuN-negative, weakly-positive, and -positive neurons, indicating that the primitive clusters extended beyond the NeuN-negative immature neuronal zone (PCZ) and that the deepest part of the

primitive clusters (lowest 2–3 cells) were positive for NeuN (Figure 4b1, orange lines outline nuclei of neurons in the presumptive primitive cluster; magenta dotted lines outline nuclei of neurons at the bottom part of the cluster; yellow color for NeuN-negative and cyan color for -positive neurons).

To investigate the incorporation of neurons into the primitive clusters, we performed time-lapse imaging after the sequential IUE experiments with a 1-day interval (Figure 5a). We first introduced an EGFP-expressing vector at E13.0 to label earlier-born neurons; then, a tdTomato-expressing vector was transfected at E14.0 to label one-day later-born neurons (Figure 5b). The time-lapse observations were started at E17.0, when the major population of the EGFP-labeled neurons had reached the outermost part of the CP. Under this live monitoring, we observed that many tdTomato-positive neurons utilized the terminal translocation mode of migration, showing a branching point (Figure 5b, yellow arrows) near the pial surface with rapid movement of the cell bodies toward the branch points (Figure 5b, orange arrowheads) (Nadarajah et al., 2001). On the other hand, most of the EGFP-labeled neurons had relocated toward the deeper part of the CP, indicating that they had indeed finished their migration after arriving at the top of the CP and had changed their relative positions to deeper inside the CP (Figure 5b, cyan arrowheads).

We then examined whether the "migrated neurons" were incorporated into the primitive neuronal clusters in a birth-date-dependent manner using brains fixed after the sequential IUE experiments with a 1-day interval. Here, we used "migrated neurons" to denote the neurons that had just finished radial migration (terminal translocation). We first introduced an EGFP-expressing vector at E14.5 to label earlier-born neurons; then, a tdTomato-expressing vector was transfected at E15.5 to label neurons born 1 day later (Figure 5c). The brains were collected at P1.0 or P2.0, once a sufficient number of EGFP- and tdTomato-labeled neurons were located in and beneath the PCZ after completing radial migration. Consistent with the observation in Figure 4, the presumptive primitive neuronal clusters consisted of both NeuN-negative (Figure 5c, yellow arrowheads), weakly-positive (Figure 5c, yellow–cyan gradient arrowheads), and -positive (Figure 5c, cyan arrowheads) neurons. At P1.0, 1-day earlier-born EGFP-labeled neurons were located more deeply within the presumptive primitive clusters than the tdTomato-labeled neurons and were weakly positive for NeuN. At P2.0, the relative topology of the EGFP- and tdTomato-labeled neurons was the same as that at P1.0 in the sense that the EGFP-labeled neurons were deeper than the tdTomato-labeled neurons. However, both of the labeled neuron types tended to be located at a greater distance from the MZ, compared with the labeled neurons at P1.0. Furthermore, the EGFP-labeled neurons were frequently round-shaped and were relatively isolated beneath the presumptive primitive clusters with NeuN-positive signals at this stage (Figure 5c, white arrowheads). These results are reasonable since, at P2.0, about 7 days had passed after IUE for the EGFP-labeled neurons and most of the labeled neurons were found beneath the PCZ with a matured status at this stage (Figures 1 and 4). Similarly, the sequential intraperitoneal injection of EdU and BrdU at a 1-day interval proved that the neurons were arranged within the PCZ in a birth-date-dependent manner (Figure 6). Together, these findings suggest that migrated neurons are incorporated sequentially into primitive neuronal clusters, resulting in an inside-out manner of neuronal alignment within the clusters and a gradual maturation as they shift to the deep side of the clusters.

3.4 | EGFP-labeled migrated neurons participate in the primitive neuronal clusters with direct cell-to-cell contact

To confirm that the newly arrived neurons at the top of the CP are incorporated into the primitive neuronal clusters, we then performed an immuno-EM analysis. To label the migrating neurons, we introduced an EGFP-expressing plasmid into the VZ cells at E14.5 and fixed the brain at E17.0 (Figure 7a,b) when the labeled neurons were still migrating. EGFP proteins were visualized with nanogold (black dots). An EGFP-labeled migrating neuron (Figure 7a, blue arrowheads) had a nucleus with a spindle shape and was found between primitive neuronal clusters (Figure 7a,a1, white arrows indicate the neurons forming a primitive cluster). Some EGFP-labeled migrating neurons were positioned between other cells separated by other structures (Figure 7b2′,b3′, marked in blue, contoured images of Figure 7b2,b3), indicating that they did not have direct contact with the clusters. When introducing an EGFP-expressing plasmid at E15.5 and fixing the brain at P1.0, the labeled neurons tended to have a round-shaped nucleus (Figure 7c). Because about 5 days had passed since IUE, the labeled neurons were supposed to have already completed migration. Highly magnified images confirmed that the labeled neuron was in direct contact with the above-positioned neuron in a primitive cluster (Figure 7c2,c2′). Along with the observation shown in Figure 4 and considering the time after IUE, these results suggest that primitive neuronal clusters are mainly composed of migrated neurons, while migrating neurons tend to pass between the clusters.

3.5 | GABAergic inhibitory interneurons are occasionally found within the primitive neuronal clusters

Since cortical neurons include both glutamatergic excitatory neurons and GABAergic inhibitory interneurons, we examined whether GABAergic inhibitory interneurons are incorporated into the presumptive primitive clusters using single optical sections under a confocal microscope. To identify the PCZ, we stained P0.5 mouse brains of GAD67-GFP mice, in which GABAergic interneurons are genetically labeled with EGFP (Tamamaki et al., 2003), with an anti-NeuN antibody (Figure 8a). Indeed, some EGFP-positive interneurons were found within the clusters (yellow arrowheads for radially assembled neurons). The EGFP-positive GABAergic interneurons in the clusters were either very weakly NeuN-positive (magenta arrows) or -positive (cyan arrows). We then performed time-lapse imaging after introducing a tdTomato-expressing vector at E14.5 in a GAD67-GFP mouse (Figure 8b). Time-lapse imaging was started at P0.5, at which time the major population of the tdTomato-labeled neurons had reached the top of the CP. Some EGFP-positive interneurons seemed to interact consistently with tdTomato-labeled neurons within the PCZ during the imaging (Figure 8b, cyan arrowheads). Other EGFP-positive interneurons seemed to interact for a shorter time than the persistently

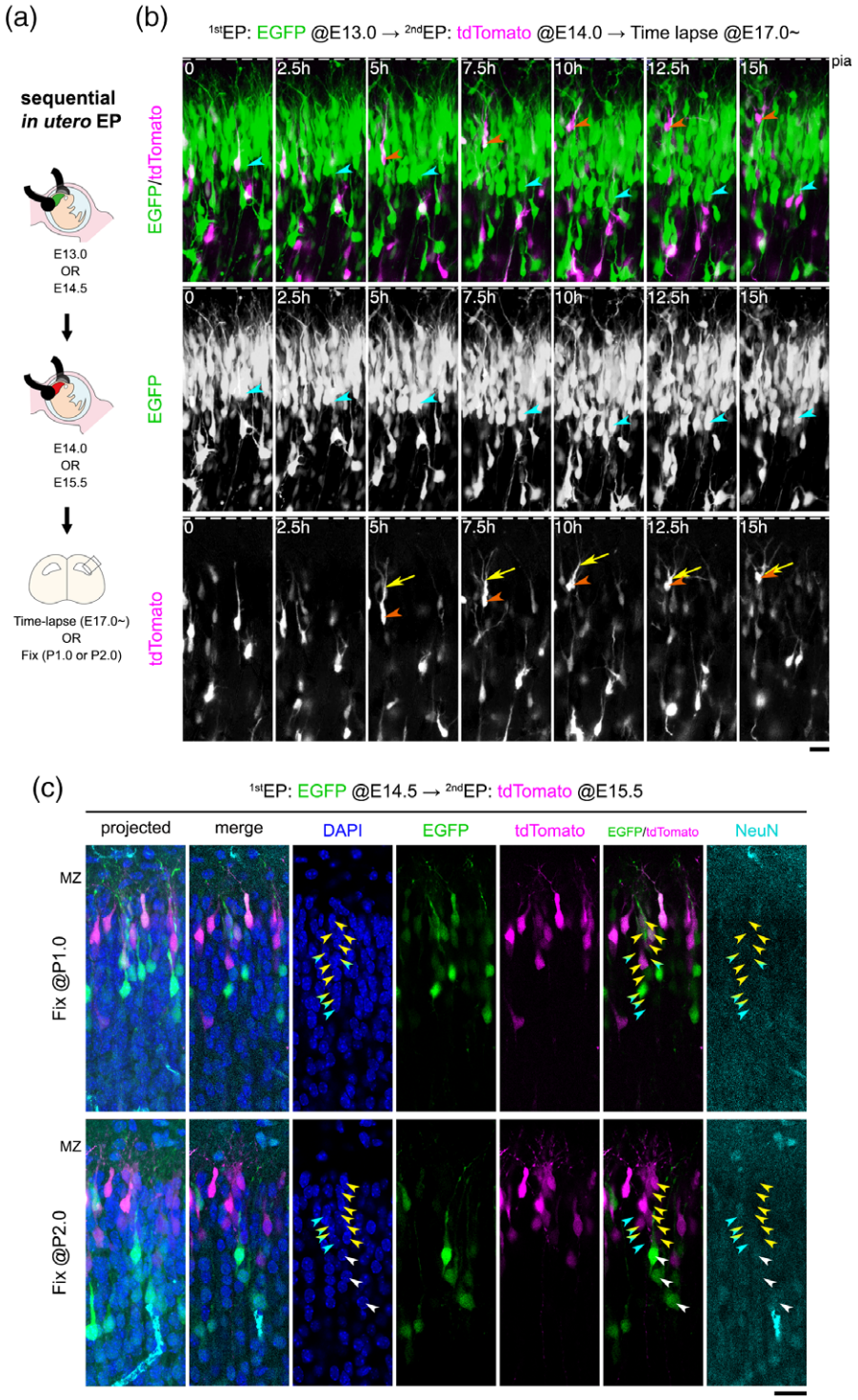

FIGURE 5 Birth-date-dependent behavior or positional changes of migrated neurons within the presumptive neuronal clusters in mouse somatosensory cortex. (a) Schematic representation of sequential *in utero* electroporation. Different fluorescent plasmids were introduced at one-day intervals. (b) Fluorescent plasmids were introduced at E13.0 (EGFP) and then at E14.0 (tdTomato). Cortical slices were prepared at E17.0, and time-lapse images were taken with a confocal microscope. An EGFP-labeled neuron that is being released from the primitive cortical zone toward the deeper part of the CP is indicated by the cyan arrowhead, and a tdTomato-labeled neuron in the process of terminal translocation is indicated by the orange arrowhead. A branching point of the tdTomato-labeled cell is shown with the yellow arrows. (c) Fluorescent plasmids were introduced at E14.5 (EGFP) and then at E15.5 (tdTomato). Cortical sections were analyzed at P1.0 and P2.0 at 1-day interval. On single optical sections, the presumptive primitive clusters were marked using yellow (NeuN negative), cyan (NeuN positive), or both (relatively weakly NeuN positive)-colored arrowheads. EGFP-positive cells observed relatively bottom part of the clusters are indicated by the white arrowheads. MZ = marginal zone. Scale bar: 20 μm

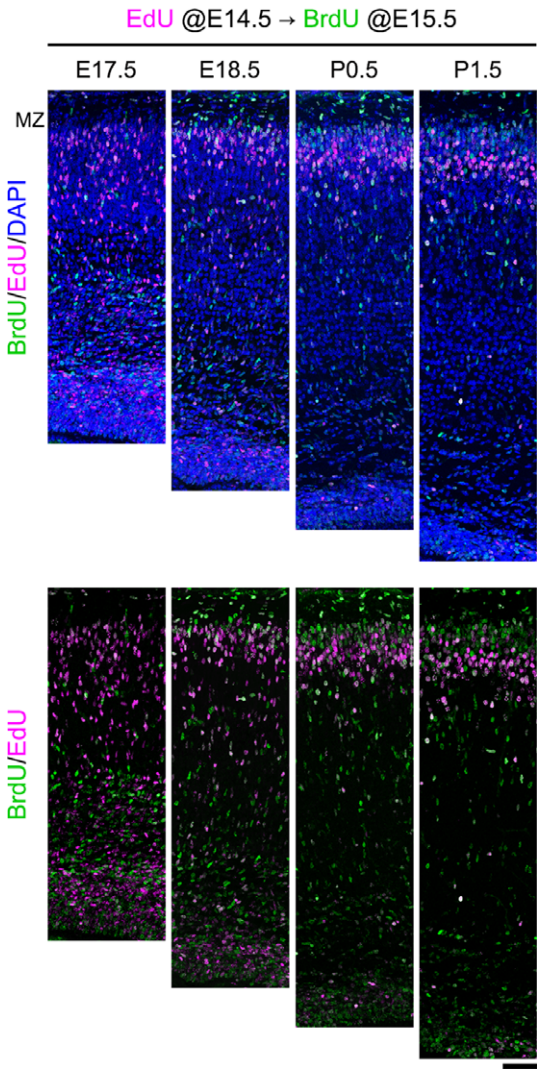

FIGURE 6 Birth-date-dependent profiles of EdU and BrdU-labeled neurons in mouse somatosensory cortex. First, EdU was introduced into pregnant mice at E14.5; BrdU was then injected on the following day (E15.5), and the brains were collected 3–7 days after EdU injection at 1-day interval. MZ = marginal zone. Scale bar: 50 μm

interacting group of cells (Figure 8b, yellow arrows). Additionally, actively migrating EGFP-positive interneurons were also detected. These results demonstrate that the some GABAergic inhibitory interneurons assemble together with migrated excitatory neurons within the PCZ.

To confirm the integration of GABAergic interneurons into the primitive neuronal clusters, we next performed an immuno-EM analysis. Primitive clusters identified by direct cell-to-cell contact were also found in the outermost region of the somatosensory cortex of P0.5 GAD67-GFP mice. Immunolabeled EGFP-positive interneurons were indeed observed within these primitive clusters (Figure 9; G1, G2, G3, and G4 indicate EGFP-positive interneurons) and were in direct contact with unlabeled excitatory neurons. Cell membrane contoured images are shown in Figure S5, Supporting Information. These results indicate that the primitive neuronal clusters are composed of both excitatory and inhibitory neurons, even though the major population of primitive clusters consists of excitatory neurons and only a portion of the clusters embrace inhibitory interneurons.

To determine the proportion of interneurons within the primitive neuronal clusters and what kinds of GABAergic interneurons were incorporated into the clusters within the PCZ in the somatosensory cortex, P0.5 GAD67-GFP mouse brains were stained with antibodies against interneuron markers (calbindin, calretinin, and Prox1; Figure 10) (Anderson et al., 1997; DeFelipe, 1997; Rubin & Kessaris, 2013). Then, we quantified the GABAergic interneuron population within the clusters (limited to the PCZ), as shown in Table 2. We counted 428 clusters in four different brains stained for calbindin, calretinin, and Prox1. Approximately 6.2 neurons were observed in a single cluster and about 0.7 EGFP-positive cells were included in each cluster. Among the clustered neurons, the proportion of EGFP-positive interneurons was about 11%. In other words, the ratio of excitatory and inhibitory neurons within the clusters was approximately 9 to 1.

Although the population size was small, calbindin-, calretinin-, or Prox1- and EGFP-double positive interneurons were observed in the presumptive primitive neuronal clusters within the PCZ (Figure 10, white arrows). Among the EGFP-positive inhibitory interneurons found in the clusters within the PCZ, calbindin-, calretinin-, and Prox1-positive interneurons occupied about 20–30% (calbindin: 33.9 ± 3.9%, calretinin: 21.1 ± 2.3%, Prox11: 26.1 ± 4.1%, Table 2). Since the proportion of Prox1-positive CGE-derived cells was around 26% and most of the remaining cells were thought to be MGE-derived cells, these results suggest that both CGE- and possibly MGE-derived inhibitory interneurons were included in the primitive neuronal clusters.

3.6 | Primitive neuronal clusters are observed in the outermost region of the CP in the developing macaque neocortex

We previously described that the PCZ-like cell dense region was also observed in the outermost region of the developing neocortex of *M. fascicularis* (Sekine et al., 2014). Macaque cortical neurogenesis occurs during E40-E100 (Dehay, Giroud, Berland, Smart, & Kennedy, 1993; Rakic, 1974, 2009; Smart, Dehay, Giroud, Berland, & Kennedy, 2002). Accordingly, neurons found in E78 macaque neocortices are still being actively generated and migrating toward the outermost region of the CP at these stages. To confirm the existence of the PCZ, defined as a zone of densely packed relatively immature neurons that are negative for NeuN (Sekine et al., 2011), we stained E78 macaque brains with an anti-NeuN antibody. When the occipital cortex of the developing macaque neocortex was examined (Figure 11), a NeuN-negative densely packed relatively immature neuronal zone (Figure 11b, cyan bar) was observed in the outermost region of the CP. Similar to the PCZ in mouse neocortex, the NeuN-negative zone was mostly coincident with the densely packed neuronal zone (Figure 11b). On a highly magnified single optical section (Figure 11c), we were able to identify radially aligned neuronal clusters beneath the MZ. Compared with mouse PCZ neurons, more immature neurons were observed in one cluster, with a height of around 10 cells. Consistent with the primitive neuronal clusters found in the mouse neocortex, NeuN-positive mature neurons were found relatively deep within

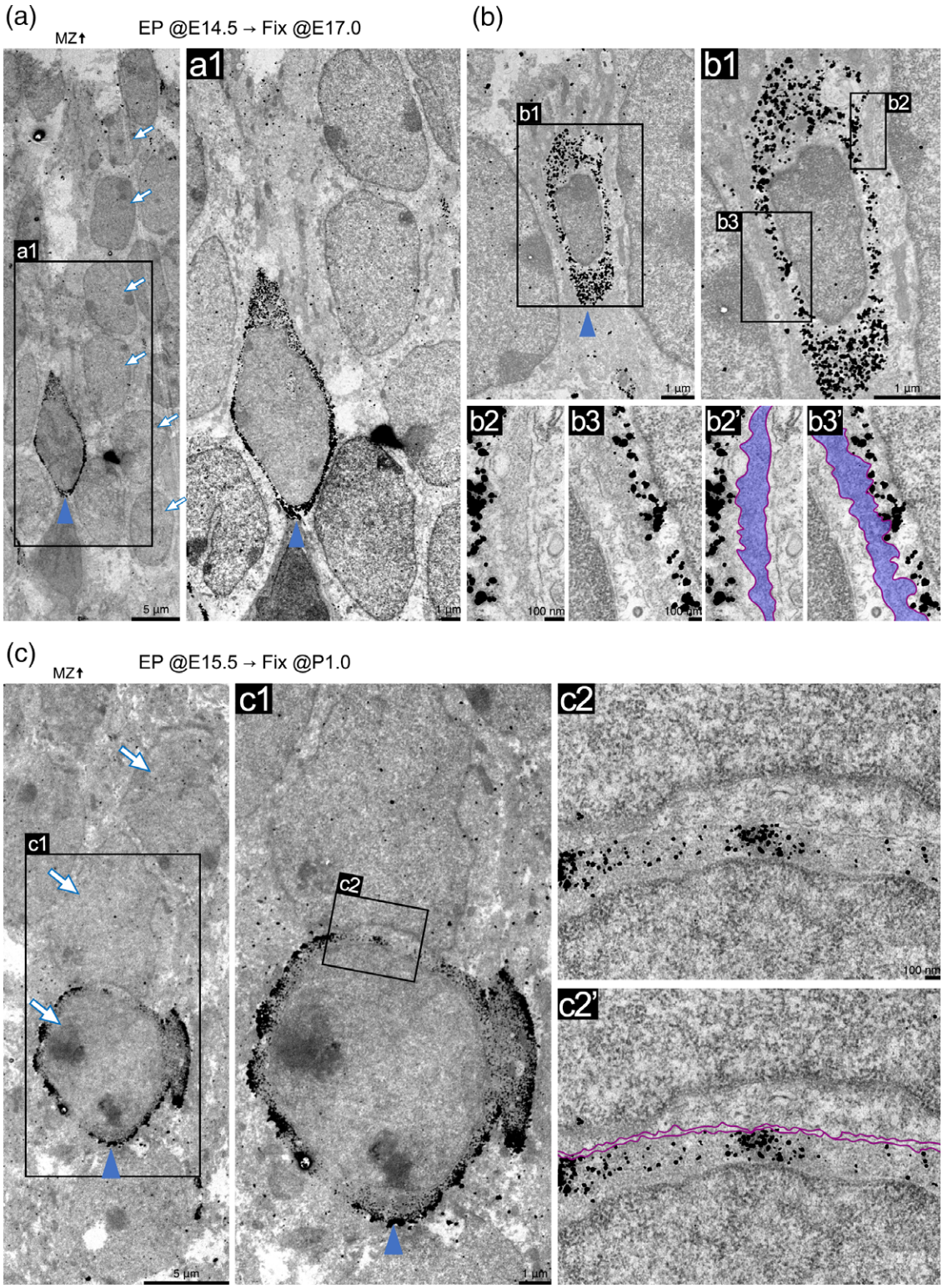

FIGURE 7 Immuno-EM images of neurons that are migrating along or incorporated into the primitive cluster in mouse somatosensory cortex. (a–c) Neurons that form a primitive cluster are indicated by the white arrows, and the immuno-stained neurons are indicated by the blue arrowheads. After the transfection of an EGFP plasmid at E14.5 or E15.5, migrating neurons (fixed at E17.0, a and b) and migrated neurons (fixed at P1.0, c) were immunolabeled with an anti-GFP antibody (visualized with nanogold, black spots). (a1, b1, and c1) Enlarged views of the boxed regions in a–c. (b2, b3) Enlarged views of the boxed regions in b1. (b2′, b3′, and c2′) Images numbered with an apostrophe are contoured images of b2, b3, and c2. The cell membranes are outlined in magenta, and the intervening structures between the contoured cells are stained blue. An EGFP-positive migrating neuron in (b) is separated from the neighboring neurons by intervening structures (blue color). (c2) Enlarged view of (c1) showing that the two cells have attached to each other. MZ = marginal zone [Color figure can be viewed at wileyonlinelibrary.com]

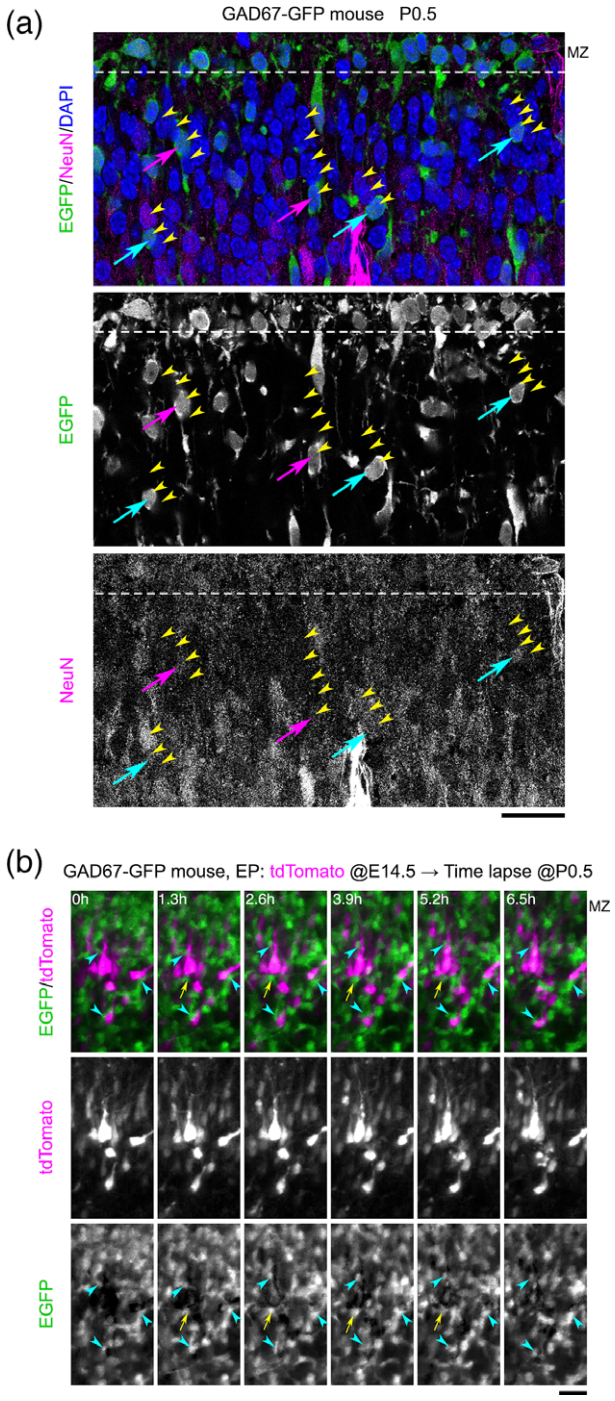

FIGURE 8 Inhibitory interneurons incorporated into some presumptive primitive neuronal clusters in GAD67-GFP mouse somatosensory cortex at P0.5. (a) The P0.5 brain of a GAD67-GFP mouse was stained with an anti-NeuN antibody. Primitive neuronal clusters (yellow arrowheads) appear to include some EGFP-positive cells on single confocal images. These EGFP-positive cells in the clusters were either weakly positive (magenta arrows) or positive (cyan arrows) for NeuN. (b) Cortical slices were prepared for time-lapse imaging at 5 days after the *in utero* electroporation (IUE) after IUE with tdTomato at E14.5. EGFP-positive neurons, which are located close to the tdTomato-labeled neuron, are indicated by the yellow arrows (short-term contact) and the cyan arrowheads (long-term contact). MZ = marginal zone. Scale bar: 25 μm

the clusters. Next, we examined GABAergic inhibitory interneurons in the clusters of the macaque neocortex. Although the numbers were small, calretinin- and Prox1-positive interneurons were detected in the presumptive primitive neuronal clusters within the PCZ on magnified single optical sections (Figure 11d). These results suggest that the primitive clustering of neurons observed in the mouse neocortex might also occur in nonhuman primate cortex, or at least in the macaque occipital cortex.

3.7 | Radially aligned neuronal clusters were also observed in the developing human neocortex

Finally, we examined the structure of the outermost region of the CP in developing human neocortex. As a reference, we first performed Nissl staining of the mouse neocortex at P0 and confirmed that primitive clusters were present at the top of the CP (Figure 12a3, cyan arrowheads). Then, human neocortex at 23 GWs was Nissl stained (Figure 12b), and we observed densely accumulated cells that resembled the mouse PCZ at the outermost region of the human neocortical CP, as previously reported (Kubo et al., 2017). Highly magnified images showed that the cells at the outermost region of the CP were radially aligned with a high cell density, forming radial arrays of cells with a height of more than 10 cells and a width of one to two cells (Figure 12b3, cyan arrowheads), resembling the primitive neuronal clusters observed in the developing mouse and macaque neocortices, while the number of neurons that participated in one cluster was larger than that in mouse neocortex. The cells beneath the presumptive primitive clusters also showed a radial columnar alignment but with lower cell densities throughout the CP (Figure 12a3,b2,b3, dashed lines). These results suggest that primitive clustering of the neurons occurs not only in the developing mouse neocortex, but also in the macaque (Figure 11) and human neocortices.

4 | DISCUSSION

In this study, we revealed that after migrating neurons in the mouse neocortex reached the top of the CP (beneath the MZ), the neurons resided within the PCZ for about 1 to 1.5 days. The PCZ was previously reported to be a densely packed cellular zone composed of relatively immature (NeuN-negative) neurons that is observed in mouse neocortex from around E16.5 to P3.5 (Sekine et al., 2011). A similar cell-dense structure has been described in human cortex as a remnant of the original undifferentiated pyramidal cell plate (PCP), while the original PCP appears at the early stage of cortical development and its structure is composed solely of pyramidal neurons (Marin-Padilla, 2011, p. 5; Marin-Padilla, 2014). Another term, the dense CP refers to a similar structure, but the dense CP differs from the PCZ in several aspects (Catalano, Robertson, & Killackey, 1991; Schlaggar & O'Leary, 1994). First, the thickness of the dense CP is larger than that of the PCZ, which is relatively constant in thickness among the different stages when this structure is observed (E16.5–P3.5). Second, the dense CP can be detected as a non-labeled zone when the thalamic afferents are labeled, while the PCZ is defined as a NeuN-negative zone. Third, according to Catalano et al. (1991), the dense CP is found in E16 rat neocortex, which corresponds to around E14 in mouse neocortex (Catalano et al., 1991). In contrast, the PCZ is initially found around E16.5 in mouse neocortex.

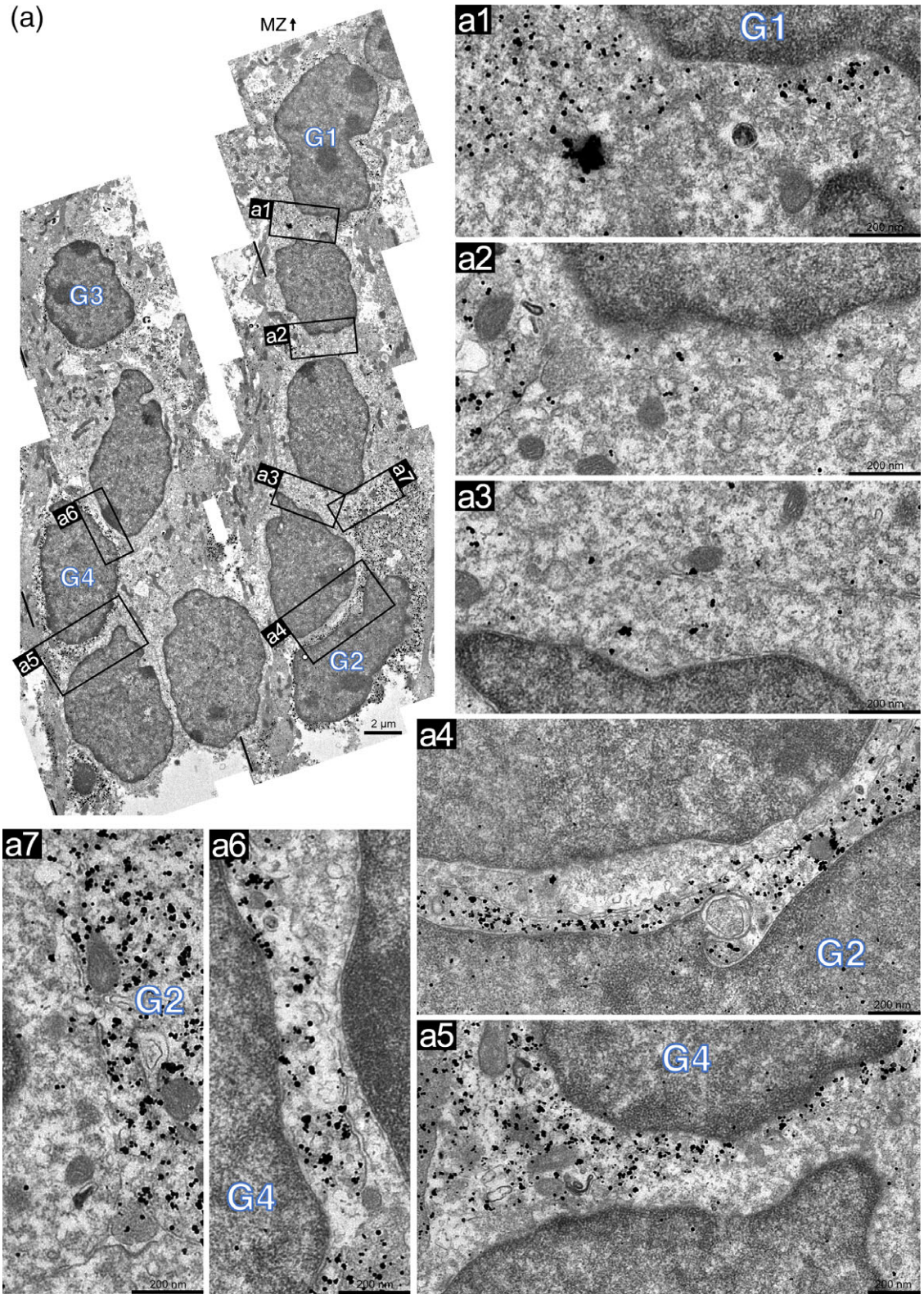

FIGURE 9 High magnified immuno-EM images of primitive neuronal clusters located beneath the MZ in GAD67-GFP mouse somatosensory cortex at P0. (a) EGFP-positive GABAergic neurons were immunolabeled with an anti-GFP antibody (visualized with nanogold, black spots). Coronal view of the neocortex beneath the MZ. Immunolabeled neurons are indicated by the white capital letters (G1–G4). (a1–a7) Enlarged views of the boxed regions in a. MZ = marginal zone [Color figure can be viewed at wileyonlinelibrary.com]

An EM analysis showed that many neurons in and below the PCZ are in direct contact with each other at their cell bodies, forming clusters (primitive neuronal clusters) mainly but not exclusively in a radial direction with a height of 3–7 cells and a width of 1–2 cells on a two-dimensional view. The primitive clusters in the mouse neocortex extended downward beyond the PCZ and were composed of both

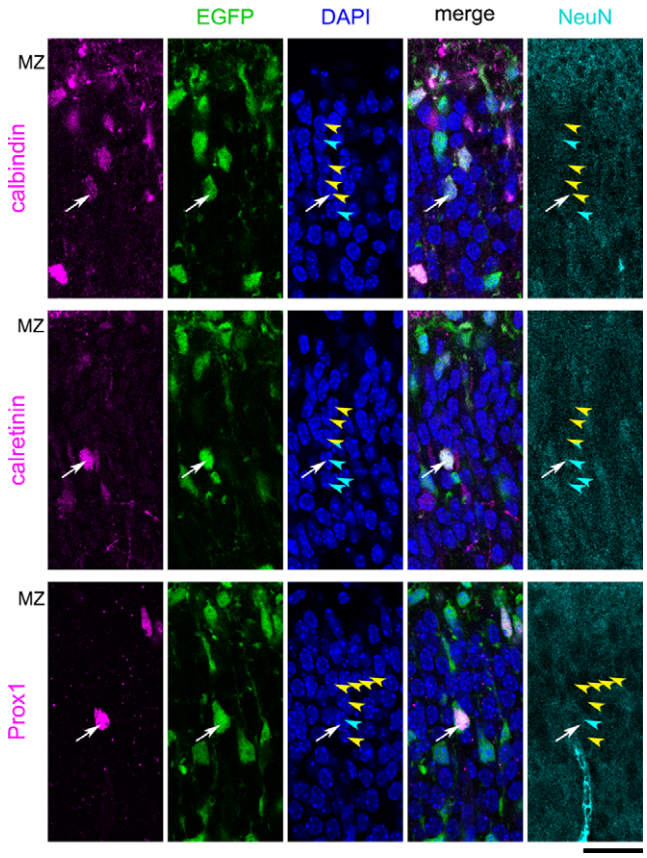

FIGURE 10 GABAergic interneuron marker- and GFP-positive neurons in GAD67-GFP mouse somatosensory cortex at P0. Brains were stained with anti-calbindin, anti-calretinin, and anti-Prox1 antibodies (magenta) and 4′,6-diamidino-2-phenylindole (DAPI; blue). Both EGFP- and calbindin-, calretinin-, or Prox1-positive neurons are indicated by the white arrows. On single optical sections, the presumptive primitive clusters were marked using yellow (NeuN negative), cyan (NeuN positive), and both (relatively weakly NeuN positive)-colored arrowheads. MZ = marginal zone. Scale bar: 25 μm

NeuN-negative immature neurons and the NeuN-positive mature neurons at the superficial region of the CP (1–3 cells). A time-course analysis of the EGFP-labeled neurons using IUE revealed that the neurons within the primitive clusters changed their location in an inside-out manner. Namely, newly arrived neurons participated in the superficial part of the primitive clusters, shifted their relative location to the deeper side, and finally left the clusters at the bottom of the structure. Considering the time course of neuronal maturation, it is conceivable that these primitive clusters are formed transiently and then gradually dissociate one-by-one into individual cells at the bottom of the structure.

How do newly incorporated neurons form clusters mainly, but not exclusively, in a radial direction? During the final step of radial migration, the tips of the leading processes of the migrating neurons are anchored to the MZ through integrin-mediated adhesion to the extracellular matrix in the MZ and N-cadherin-mediated interaction with Cajal–Retzius cells, while the cell bodies are still located below or within the PCZ (Franco, Martinez-Garay, Gil-Sanz, Harkins-Perry, & Muller, 2011; Gil-Sanz et al., 2013; Sekine et al., 2011; Sekine et al., 2012; Tachikawa, Sasaki, Maeda, & Nakajima, 2008; Weber, Bjerke, & DeSimone, 2011). During this process, cell bodies are thought to detach from the radial fibers and translocate quickly toward the outermost region of the CP, eventually terminating their radial migration (Sekine et al., 2014). After the neurons stop at the top of the CP, they are passed by later-born neurons, resulting in an inside-out manner of neuronal alignment. How the earlier-born neurons allow the later-born neurons to insert themselves between the earlier-born neurons and the MZ, leading to an inside-out alignment, is not yet clearly understood. However, this process is known to be accompanied by the elongation of the apical dendrites and the gradual maturation of the neurons (Marin-Padilla, 1992). Interestingly, we found in this study that the apical dendrites of the later-born neurons extend toward the MZ along with the apical dendrites of the earlier-born neurons within the same primitive clusters (Figure 4a,b1), suggesting that preexisting neuronal processes could provide later-born neurons with a proper route for their relocation, thereby promoting the formation of a radial arrangement of neurons within the primitive clusters. In another possible scenario, the incorporation of the later-born neurons into the top of the primitive cluster might promote the extension of the apical dendrites of the earlier-born neurons. However, we cannot exclude the possibility that these two events might occur only correlatively, and not causally. It might also be possible that some physical force such as that

TABLE 2 EGFP-positive GABAergic interneuron population within primitive neuronal clusters in somatosensory cortex of GAD67-GFP mouse at P0

	Number or percentage (%)			
	EGFP	calbindin	calretinin	Prox1
Total number of counted clusters (=a)	428	139	162	127
Total number of counted cells in clusters (=b)	2,680	849	1,004	827
Number of counted cells in clusters/counted clusters (=b/a)[a]	6.2 ± 0.2			
Total number of counted EGFP-positive cells in clusters (=c)	303	98	97	108
Number of EGFP-positive cells in clusters/counted clusters (=c/a)[a]	0.7 ± 0.1			
Percentage of EGFP-positive cells in clusters/counted cells in clusters (=c/b) (%)[a]	11.1 ± 1.1			
Total number of counted marker-positive cells in clusters (=d)		32	19	31
Number of counted marker-positive cells in clusters/counted clusters (=d/a)[a]		0.2 ± 0.0	0.1 ± 0.0	0.2 ± 0.0
Percentage of counted marker-positive cells in clusters/counted EGFP-positive cells in clusters (=d/c) (%)[a]		33.9 ± 3.9	21.1 ± 2.3	26.1 ± 4.1

[a] Plus–minus values are means ± *SD* (*n* = 4 brains).

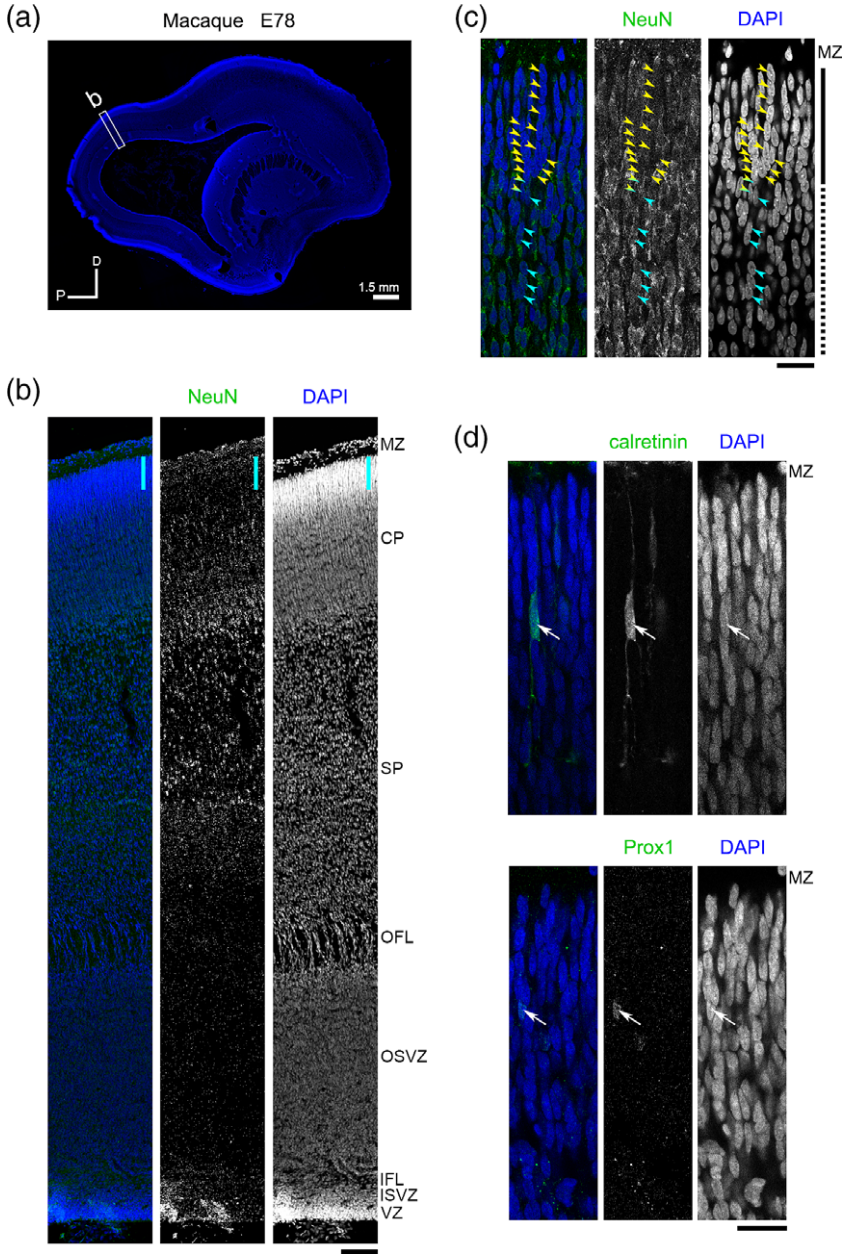

FIGURE 11 Presumptive primitive neuronal clusters found at the outermost region of E78 macaque occipital cortex. (a, b) 4′,6-Diamidino-2-phenylindole (DAPI)-stained parasagittal section of an E78 macaque fetal brain. (b) Enlarged view of the boxed region in a (Area 17 in occipital cortex). The brain was stained with an anti-NeuN antibody and DAPI. The primitive cortical zone (PCZ) is indicated by the cyan bars. Scale bar: 100 μm. (c) On magnified single optical sections, radially aligned, presumptive primitive neuronal clusters can be identified using DAPI staining (yellow arrowheads for NeuN-negative neurons, cyan for NeuN-positive neurons, and both for weakly NeuN-positive neurons). The PCZ is indicated by the thick black line next to the figure. Scale bar: 25 μm. (d) The brain was stained with anti-calbindin and anti-Prox1 antibodies and DAPI. Calbindin- and calretinin-positive neurons are indicated by the yellow arrows. Scale bar: 25 μm. CP = cortical plate; D = dorsal; IFL = inner fiber layer; ISVZ = inner subventricular zone; MZ = marginal zone; OFL = outer fiber layer; OSVZ = outer subventricular zone; P = posterior; SP = subplate; VZ = ventricular zone

generated by extending axons that pull down or "anchor" themselves, especially cells near the bottom of the primitive clusters, might enable later-born neurons to insert themselves between the clusters and the MZ. Further investigation of how this transient neuronal clustering occurs and how neurons leave this cluster upon maturation is needed.

Of note, the neurons that form the primitive clusters are composed of not only excitatory neurons, but also GABAergic inhibitory interneurons. Inhibitory interneurons originating from progenitors within the germinal zones of the ventral telencephalon migrate tangentially and then radially to become allocated to the developing CP. Among two large migratory streams, MZ and SVZ, SST+ Martinotti and PV+ interneurons preferentially migrate through the MZ (Lim, Mi, Llorca, & Marin, 2018). Martinotti cells are known to be positive for the calcium-binding proteins calbindin and calretinin and are abundant in Layer 5 or Layers 2/3. In addition, VIP+ interneurons, which are enriched in Layer 2/3, often coexpress calretinin. The incorporation of interneurons to the CP consistently occurs until postnatal

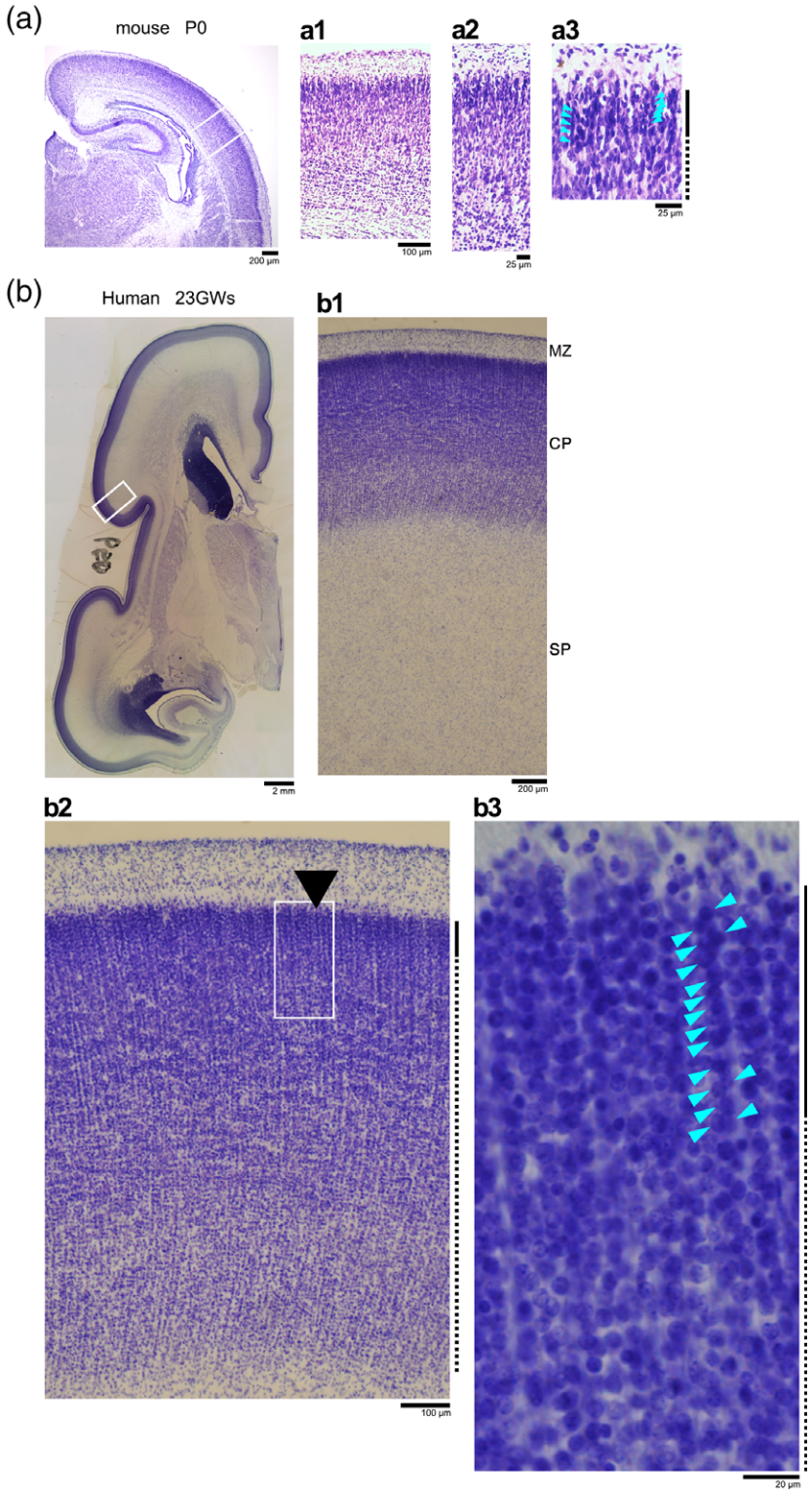

FIGURE 12 Radially aligned neurons in mouse and human neocortices. (a, a1, a2, and a3) A mouse P0 brain was stained with Nissl, and enlarged images are shown on the right. (b, b1, b2, and b3) A 23GW human brain was stained with Nissl. Enlarged images are shown on the right. (a1, b1, and b3) The white rectangle regions are enlarged in a, b and b2, respectively. (a3, b2, and b3) The densely packed neuronal zone is shown by the black line. The black dashed lines extend to the CP. (a3, b3) Cyan arrowheads show radially aligned presumptive primitive clusters within the primitive cortical zone. CP = cortical plate; MZ = marginal zone; SP = subplate [Color figure can be viewed at wileyonlinelibrary.com]

stages in mice (Lim et al., 2018). Furthermore, CGE-derived interneurons are disposed to target superficial layers regardless of their birth date (Miyoshi et al., 2010; Miyoshi & Fishell, 2011). Compatible with these previous studies, the present study showed that calbindin, calretinin, and Prox1-positive neurons were found in the primitive neuronal clusters in the somatosensory cortex of GAD67-GFP mice at P0.5. Importantly, interactions between excitatory neurons (migrated from the VZ) and GFP-positive interneurons were suggested by the results of an EM analysis, time-lapse imaging, and an immunohistochemical analysis performed at this stage (Figures 8–10). Since several lines of

evidence indicate that pyramidal cells are responsible for the invasion of interneurons to the appropriate layers (Hevner, Daza, Englund, Kohtz, & Fink, 2004; Pla, Borrell, Flames, & Marin, 2006), the interaction between excitatory neurons and inhibitory interneurons observed within the primitive neuronal clusters might provide positional cues to the inhibitory interneurons. The possibility that this interaction might also influence the excitatory neurons cannot be excluded because newly migrated excitatory neurons residing in the outermost region of the CP have not yet completely differentiated/matured into specific subtypes at this stage. Moreover, the final settlement or differentiation of some inhibitory interneurons might be accelerated by the incorporation of the interneurons into the clusters.

A radial columnar structure of cells in the fully developed cat somatosensory cortex was found more than 60 years ago and was described as a "column" (Mountcastle, Berman, & Davies, 1955) to explain an elementary unit of organization in the neocortex (Buxhoeveden & Casanova, 2002; Favorov & Diamond, 1990; Favorov & Kelly, 1994; Jones, 2000; Lee & Whitsel, 1992; Mountcastle, 1957, 1997; Mountcastle, Davies, & Berman, 1957; Wilson, Scalaidhe, & Goldman-Rakic, 1993). Since then, various types of "columns" have been described to indicate different "columnar" structures in numerous cortex areas within several mammalian species (Molnar, 2013, p. 112–113). It is now widely accepted that the anatomical and functional columnarity of the neocortex differs dramatically in size, cell composition, synaptic organization, and other characteristics (Rakic, 2008). On the other hand, Rakic (1988), described the embryonic columnar arrangement as an "ontogenetic column," highlighting the relationship of the progenitor cells to the radial stacks of cells (radial unit hypothesis). The radial arrangement of cells in the "ontogenetic column" during neocortical development (Kostovic-Knezevic, Kostovic, Krmpotic-Nemanic, Kelovic, & Vukovic, 1978; Rakic, 1972, 1978, 1988) resembles the embryonic primitive clusters described in this study. "Primitive neuronal clusters," which extends downward beyond the PCZ, are observed in the developing cerebral neocortices of at least three different mammalian species: mouse neocortex (somatosensory cortex), macaque neocortex (occipital cortex), and human neocortex. Furthermore, many primitive clusters include not only excitatory neurons, but also inhibitory interneurons (Figures 8–11). It is thus important to clarify the relationship between "ontogenetic columns" and primitive clusters in the future. It is possible that primitive clusters ultimately develop into the "minicolumns" found in the adult neocortex. Future analyses such as tracking neurons that have participated in primitive clusters, ideally using primates, will enable us to elucidate whether radially arranged primitive clusters subsequently develop into the "minicolumns" observed in mature neocortex.

In the developing macaque and human neocortices, similar but taller primitive clusters were observed, compared with those in mice (Figures 11 and 12). If the formation of a radially aligned cellular arrangement contributes to the development of a functional unit, the larger number of cells that participate in the radial structure in macaque and human neocortices might increase the complexity of a single functional unit, possibly leading to the evolution of the functional column in the primate neocortex.

ACKNOWLEDGMENTS

The authors are grateful to the members of Nakajima Laboratory for the valuable discussions and technical support. The authors would like to thank Dr. Jun-Ichi Miyazaki for providing the plasmid (pCAGGS vector) and Dr. Hiroyuki Sakagami, Dr. Masahiro Fukaya (Kitasato University), and Dr. Toshihiro Nagai (Keio University School of Medicine) for their support and valuable comments regarding the EM analysis. The authors would also like to thank B. Beneyton, for the nonhuman primate care, M. Dirheimer and P. Misery for their expert surgical assistance, and V. Cortay for help with the histology.

CONFLICT OF INTEREST

The authors declare no conflict of interest.

ORCID

Minkyung Shin https://orcid.org/0000-0003-4156-012X
Colette Dehay https://orcid.org/0000-0002-5196-1464
Ken-ichiro Kubo https://orcid.org/0000-0003-4023-5069
Kazunori Nakajima https://orcid.org/0000-0003-1864-9425

REFERENCES

Ajioka, I., & Nakajima, K. (2005). Birth-date-dependent segregation of the mouse cerebral cortical neurons in reaggregation cultures. *The European Journal of Neuroscience*, *22*(2), 331–342. https://doi.org/10.1111/j.1460-9568.2005.04214.x

Anderson, S. A., Eisenstat, D. D., Shi, L., & Rubenstein, J. L. (1997). Interneuron migration from basal forebrain to neocortex: Dependence on Dlx genes. *Science*, *278*(5337), 474–476.

Angevine, J. B., Jr., & Sidman, R. L. (1961). Autoradiographic study of cell migration during histogenesis of cerebral cortex in the mouse. *Nature*, *192*, 766–768.

Bar, I., Lambert De Rouvroit, C., Royaux, I., Krizman, D. B., Dernoncourt, C., Ruelle, D., … Goffinet, A. M. (1995). A YAC contig containing the reeler locus with preliminary characterization of candidate gene fragments. *Genomics*, *26*(3), 543–549.

Buxhoeveden, D. P., & Casanova, M. F. (2002). The minicolumn and evolution of the brain. *Brain, Behavior and Evolution*, *60*(3), 125–151. https://doi.org/10.1159/000065935

Catalano, S. M., Robertson, R. T., & Killackey, H. P. (1991). Early ingrowth of thalamocortical afferents to the neocortex of the prenatal rat. *Proceedings of the National Academy of Sciences of the United States of America*, *88*(8), 2999–3003.

Caviness, V. S., Jr., & Sidman, R. L. (1973). Time of origin or corresponding cell classes in the cerebral cortex of normal and reeler mutant mice: An autoradiographic analysis. *The Journal of Comparative Neurology*, *148*(2), 141–151.

D'Arcangelo, G., Miao, G. G., Chen, S. C., Soares, H. D., Morgan, J. I., & Curran, T. (1995). A protein related to extracellular matrix proteins deleted in the mouse mutant reeler. *Nature*, *374*(6524), 719–723. https://doi.org/10.1038/374719a0

DeFelipe, J. (1997). Types of neurons, synaptic connections and chemical characteristics of cells immunoreactive for calbindin-D28K, parvalbumin and calretinin in the neocortex. *Journal of Chemical Neuroanatomy*, *14*(1), 1–19.

Dehay, C., Giroud, P., Berland, M., Smart, I., & Kennedy, H. (1993). Modulation of the cell cycle contributes to the parcellation of the primate visual cortex. *Nature*, *366*(6454), 464–466.

Favorov, O. V., & Diamond, M. E. (1990). Demonstration of discrete place-defined columns--segregates--in the cat SI. *The Journal of Comparative Neurology*, *298*(1), 97–112. https://doi.org/10.1002/cne.902980108

Favorov, O. V., & Kelly, D. G. (1994). Minicolumnar organization within somatosensory cortical segregates: I. Development of afferent connections. *Cerebral Cortex*, *4*(4), 408–427.

Franco, S. J., Martinez-Garay, I., Gil-Sanz, C., Harkins-Perry, S. R., & Muller, U. (2011). Reelin regulates cadherin function via Dab1/Rap1 to control neuronal migration and lamination in the neocortex. *Neuron*, *69* (3), 482–497. https://doi.org/10.1016/j.neuron.2011.01.003

Gil-Sanz, C., Franco, S. J., Martinez-Garay, I., Espinosa, A., Harkins-Perry, S., & Muller, U. (2013). Cajal-Retzius cells instruct neuronal migration by coincidence signaling between secreted and contact-dependent guidance cues. *Neuron*, *79*(3), 461–477. https://doi.org/10.1016/j.neuron.2013.06.040

Greig, L. C., Woodworth, M. B., Galazo, M. J., Padmanabhan, H., & Macklis, J. D. (2013). Molecular logic of neocortical projection neuron specification, development and diversity. *Nature Reviews Neuroscience*, *14*(11), 755–769. https://doi.org/10.1038/nrn3586

Hatanaka, Y., Hisanaga, S., Heizmann, C. W., & Murakami, F. (2004). Distinct migratory behavior of early- and late-born neurons derived from the cortical ventricular zone. *The Journal of Comparative Neurology*, *479* (1), 1–14.

Hayashi, K., Inoue, S., & Nakajima, K. (2018). Reelin. In S. Choi (Ed.), *Encyclopedia of signaling molecules*. New York, NY: Springer.

Hevner, R. F., Daza, R. A., Englund, C., Kohtz, J., & Fink, A. (2004). Postnatal shifts of interneuron position in the neocortex of normal and reeler mice: Evidence for inward radial migration. *Neuroscience*, *124*(3), 605–618.

Hirota, Y., Kubo, K., Fujino, T., Yamamoto, T. T., & Nakajima, K. (2018). ApoER2 controls not only neuronal migration in the intermediate zone but also termination of migration in the developing cerebral cortex. *Cerebral Cortex*, *28*(1), 223–235. https://doi.org/10.1093/cercor/bhw369

Hirota, Y., & Nakajima, K. (2017). Control of neuronal migration and aggregation by Reelin signaling in the developing cerebral cortex. *Frontiers in Cell and Development Biology*, *5*, 40. https://doi.org/10.3389/fcell.2017.00040

Honda, T., Kobayashi, K., Mikoshiba, K., & Nakajima, K. (2011). Regulation of cortical neuron migration by the Reelin signaling pathway. *Neurochemical Research*, *36*(7), 1270–1279. https://doi.org/10.1007/s11064-011-0407-4

Ishii, K., Kubo, K., Endo, T., Yoshida, K., Benner, S., Ito, Y., … Nakajima, K. (2015). Neuronal heterotopias affect the activities of distant brain areas and lead to behavioral deficits. *The Journal of Neuroscience*, *35* (36), 12432–12445. https://doi.org/10.1523/JNEUROSCI.3648-14.2015

Jones, E. G. (2000). Microcolumns in the cerebral cortex. *Proceedings of the National Academy of Sciences of the United States of America*, *97*(10), 5019–5021.

Kitazawa, A., Kubo, K., Hayashi, K., Matsunaga, Y., Ishii, K., & Nakajima, K. (2014). Hippocampal pyramidal neurons switch from a multipolar migration mode to a novel "climbing" migration mode during development. *The Journal of Neuroscience*, *34*(4), 1115–1126. https://doi.org/10.1523/JNEUROSCI.2254-13.2014

Kohno, T., Honda, T., Kubo, K., Nakano, Y., Tsuchiya, A., Murakami, T., … Hattori, M. (2015). Importance of Reelin C-terminal region in the development and maintenance of the postnatal cerebral cortex and its regulation by specific proteolysis. *The Journal of Neuroscience*, *35*(11), 4776–4787. https://doi.org/10.1523/JNEUROSCI.4119-14.2015

Kostovic-Knezevic, L., Kostovic, I., Krmpotic-Nemanic, J., Kelovic, Z., & Vukovic, B. (1978). The cortical plate of the human neocortex during the early fetal period (at 31-65 mm CRL). *Verhandlungen der Anatomischen Gesellschaft*, *72*, 721–723.

Kubo, K., Honda, T., Tomita, K., Sekine, K., Ishii, K., Uto, A., … Nakajima, K. (2010). Ectopic Reelin induces neuronal aggregation with a normal birthdate-dependent "inside-out" alignment in the developing neocortex. *The Journal of Neuroscience*, *30*(33), 10953–10966. https://doi.org/10.1523/JNEUROSCI.0486-10.2010

Kubo, K., Deguchi, K., Nagai, T., Ito, Y., Yoshida, K., Endo, T., … Nakajima, K. (2017). Association of impaired neuronal migration with cognitive deficits in extremely preterm infants. *JCI Insight*, *2*(10), e88609. https://doi.org/10.1172/jci.insight.88609

Lee, C. J., & Whitsel, B. L. (1992). Mechanisms underlying somatosensory cortical dynamics: I. in vivo studies. *Cerebral Cortex*, *2*(2), 81–106.

Lim, L., Mi, D., Llorca, A., & Marin, O. (2018). Development and functional diversification of cortical interneurons. *Neuron*, *100*(2), 294–313. https://doi.org/10.1016/j.neuron.2018.10.009

Lukaszewicz, A., Savatier, P., Cortay, V., Giroud, P., Huissoud, C., Berland, M., … Dehay, C. (2005). G1 phase regulation, area-specific cell cycle control, and cytoarchitectonics in the primate cortex. *Neuron*, *47*(3), 353–364. doi:S0896-6273(05)00566-0 [pii]. https://doi.org/10.1016/j.neuron.2005.06.032

Marin-Padilla, M. (1992). Ontogenesis of the pyramidal cell of the mammalian neocortex and developmental cytoarchitectonics: A unifying theory. *The Journal of Comparative Neurology*, *321*(2), 223–240. https://doi.org/10.1002/cne.903210205

Marin-Padilla, M. (2011). *The human brain: Prenatal development and structure*. Heidelberg: Springer. https://doi.org/10.1007/978-3-642-14724-1

Marin-Padilla, M. (2014). The mammalian neocortex new pyramidal neuron: A new conception. *Frontiers in Neuroanatomy*, *7*, 51. https://doi.org/10.3389/fnana.2013.00051

Matsunaga, Y., Noda, M., Murakawa, H., Hayashi, K., Nagasaka, A., Inoue, S., … Nakajima, K. (2017). Reelin transiently promotes N-cadherin-dependent neuronal adhesion during mouse cortical development. *Proceedings of the National Academy of Sciences of the United States of America*, *114*(8), 2048–2053. https://doi.org/10.1073/pnas.1615215114

Miyoshi, G., & Fishell, G. (2011). GABAergic interneuron lineages selectively sort into specific cortical layers during early postnatal development. *Cerebral Cortex*, *21*(4), 845–852. doi:bhq155 [pii]. https://doi.org/10.1093/cercor/bhq155

Miyoshi, G., Hjerling-Leffler, J., Karayannis, T., Sousa, V. H., Butt, S. J., Battiste, J., … Fishell, G. (2010). Genetic fate mapping reveals that the caudal ganglionic eminence produces a large and diverse population of superficial cortical interneurons. *The Journal of Neuroscience*, *30*(5), 1582–1594. doi:30/5/1582 [pii]. https://doi.org/10.1523/JNEUROSCI.4515-09.2010

Molnar, Z. (2013). Cortical columns. In J. L. R. Rubenstein & P. Rakic (Eds.), *Neural circuit development and function in the brain Comprehensive developmental neuroscience* (Vol. 3, pp. 109–129). Amsterdam: Elseiver.

Mountcastle, V., Berman, A., & Davies, P. (1955). Topographic organization and modality representation in first somatic area of cat's cerebral cortex by method of single unit analysis. *American Journal of Physiology*, *183*, 646.

Mountcastle, V. B. (1957). Modality and topographic properties of single neurons of cat's somatic sensory cortex. *Journal of Neurophysiology*, *20* (4), 408–434. https://doi.org/10.1152/jn.1957.20.4.408

Mountcastle, V. B. (1997). The columnar organization of the neocortex. *Brain*, *120*(Pt. 4), 701–722.

Mountcastle, V. B., Davies, P. W., & Berman, A. L. (1957). Response properties of neurons of cat's somatic sensory cortex to peripheral stimuli. *Journal of Neurophysiology*, *20*(4), 374–407. https://doi.org/10.1152/jn.1957.20.4.374

Nadarajah, B., Brunstrom, J. E., Grutzendler, J., Wong, R. O., & Pearlman, A. L. (2001). Two modes of radial migration in early development of the cerebral cortex. *Nature Neuroscience*, *4*(2), 143–150.

Nakajima, K., Mikoshiba, K., Miyata, T., Kudo, C., & Ogawa, M. (1997). Disruption of hippocampal development in vivo by CR-50 mAb against Reelin. *Proceedings of the National Academy of Sciences of the United States of America*, *94*(15), 8196–8201. https://doi.org/10.1073/Pnas.94.15.8196

Noctor, S. C., Martinez-Cerdeno, V., Ivic, L., & Kriegstein, A. R. (2004). Cortical neurons arise in symmetric and asymmetric division zones and migrate through specific phases. *Nature Neuroscience*, *7*(2), 136–144.

Ogawa, M., Miyata, T., Nakajima, K., Yagyu, K., Seike, M., Ikenaka, K., … Mikoshiba, K. (1995). The reeler gene-associated antigen on Cajal-Retzius neurons is a crucial molecule for laminar organization of cortical neurons. *Neuron*, *14*(5), 899–912.

Pla, R., Borrell, V., Flames, N., & Marin, O. (2006). Layer acquisition by cortical GABAergic interneurons is independent of Reelin signaling. *The Journal of Neuroscience*, *26*(26), 6924–6934.

Rakic, P. (1972). Mode of cell migration to the superficial layers of fetal monkey neocortex. *The Journal of Comparative Neurology*, *145*(1), 61–83. https://doi.org/10.1002/cne.901450105

Rakic, P. (1974). Neurons in rhesus monkey visual cortex: Systematic relation between time of origin and eventual disposition. *Science*, *183* (4123), 425–427.

Rakic, P. (1978). Neuronal migration and contact guidance in the primate telencephalon. *Postgraduate Medical Journal*, *54*(Suppl. 1), 25–40.

Rakic, P. (1988). Specification of cerebral cortical areas. *Science*, *241* (4862), 170–176.

Rakic, P. (2008). Confusing cortical columns. *Proceedings of the National Academy of Sciences of the United States of America*, *105*(34), 12099–12100. https://doi.org/10.1073/pnas.0807271105

Rakic, P. (2009). Evolution of the neocortex: A perspective from developmental biology. *Nature Reviews. Neuroscience*, *10*(10), 724–735. https://doi.org/10.1038/nrn2719

Rubin, A. N., & Kessaris, N. (2013). PROX1: A lineage tracer for cortical interneurons originating in the lateral/caudal ganglionic eminence and preoptic area. *PLoS One*, *8*(10), e77339. https://doi.org/10.1371/journal.pone.0077339

Rymar, V. V., & Sadikot, A. F. (2007). Laminar fate of cortical GABAergic interneurons is dependent on both birthdate and phenotype. *The Journal of Comparative Neurology*, *501*(3), 369–380. https://doi.org/10.1002/cne.21250

Schlaggar, B. L., & O'Leary, D. D. (1994). Early development of the somatotopic map and barrel patterning in rat somatosensory cortex. *The Journal of Comparative Neurology*, *346*(1), 80–96. https://doi.org/10.1002/cne.903460106

Sekine, K., Honda, T., Kawauchi, T., Kubo, K., & Nakajima, K. (2011). The outermost region of the developing cortical plate is crucial for both the switch of the radial migration mode and the Dab1-dependent "inside-out" lamination in the neocortex. *The Journal of Neuroscience*, *31*(25), 9426–9439. https://doi.org/10.1523/JNEUROSCI.0650-11.2011

Sekine, K., Kawauchi, T., Kubo, K., Honda, T., Herz, J., Hattori, M., … Nakajima, K. (2012). Reelin controls neuronal positioning by promoting cell-matrix adhesion via inside-out activation of integrin alpha5beta1. *Neuron*, *76*(2), 353–369. https://doi.org/10.1016/j.neuron.2012.07.020

Sekine, K., Kubo, K., & Nakajima, K. (2014). How does Reelin control neuronal migration and layer formation in the developing mammalian neocortex? *Neuroscience Research*, *86*, 50–58. https://doi.org/10.1016/j.neures.2014.06.004

Smart, I. H., Dehay, C., Giroud, P., Berland, M., & Kennedy, H. (2002). Unique morphological features of the proliferative zones and postmitotic compartments of the neural epithelium giving rise to striate and extrastriate cortex in the monkey. *Cerebral Cortex*, *12*(1), 37–53.

Tabata, H., Kanatani, S., & Nakajima, K. (2009). Differences of migratory behavior between direct progeny of apical progenitors and basal progenitors in the developing cerebral cortex. *Cerebral Cortex*, *19*(9), 2092–2105. https://doi.org/10.1093/cercor/bhn227

Tabata, H., & Nakajima, K. (2001). Efficient *in utero* gene transfer system to the developing mouse brain using electroporation: Visualization of neuronal migration in the developing cortex. *Neuroscience*, *103*(4), 865–872.

Tabata, H., & Nakajima, K. (2003). Multipolar migration: The third mode of radial neuronal migration in the developing cerebral cortex. *The Journal of Neuroscience*, *23*(31), 9996–10001.

Tabata, H., & Nakajima, K. (2008). Labeling embryonic mouse central nervous system cells by *in utero* electroporation. *Development, Growth & Differentiation*, *50*(6), 507–511. https://doi.org/10.1111/j.1440-169X.2008.01043.x

Tachikawa, K., Sasaki, S., Maeda, T., & Nakajima, K. (2008). Identification of molecules preferentially expressed beneath the marginal zone in the developing cerebral cortex. *Neuroscience Research*, *60*(2), 135–146. https://doi.org/10.1016/j.neures.2007.10.006

Tamamaki, N., Yanagawa, Y., Tomioka, R., Miyazaki, J., Obata, K., & Kaneko, T. (2003). Green fluorescent protein expression and colocalization with calretinin, parvalbumin, and somatostatin in the GAD67-GFP knock-in mouse. *The Journal of Comparative Neurology*, *467*(1), 60–79.

Tan, X., & Shi, S. H. (2013). Neocortical neurogenesis and neuronal migration. *Wiley Interdisciplinary Reviews: Developmental Biology*, *2*(4), 443–459. https://doi.org/10.1002/wdev.88

Taniguchi, H., Lu, J., & Huang, Z. J. (2013). The spatial and temporal origin of chandelier cells in mouse neocortex. *Science*, *339*(6115), 70–74. https://doi.org/10.1126/science.1227622

Weber, G. F., Bjerke, M. A., & DeSimone, D. W. (2011). Integrins and cadherins join forces to form adhesive networks. *Journal of Cell Science*, *124*(Pt. 8), 1183–1193. https://doi.org/10.1242/jcs.064618

Wilson, F. A., Scalaidhe, S. P., & Goldman-Rakic, P. S. (1993). Dissociation of object and spatial processing domains in primate prefrontal cortex. *Science*, *260*(5116), 1955–1958.

Yozu, M., Tabata, H., & Nakajima, K. (2004). Birth-date dependent alignment of GABAergic neurons occurs in a different pattern from that of non-GABAergic neurons in the developing mouse visual cortex. *Neuroscience Research*, *49*(4), 395–403. https://doi.org/10.1016/j.neures.2004.05.005

SUPPORTING INFORMATION

Additional supporting information may be found online in the Supporting Information section at the end of the article.

How to cite this article: Shin M, Kitazawa A, Yoshinaga S, et al. Both excitatory and inhibitory neurons transiently form clusters at the outermost region of the developing mammalian cerebral neocortex. *J Comp Neurol*. 2019;1–21. https://doi.org/10.1002/cne.24634